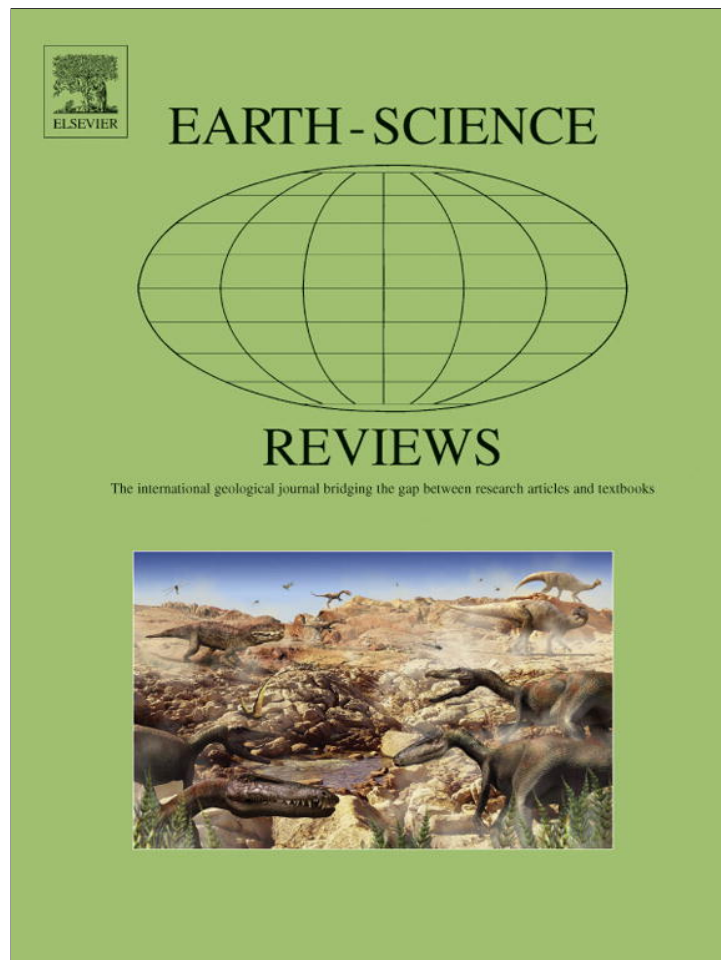


Provided for non-commercial research and education use.
Not for reproduction, distribution or commercial use.



This article appeared in a journal published by Elsevier. The attached copy is furnished to the author for internal non-commercial research and education use, including for instruction at the authors institution and sharing with colleagues.

Other uses, including reproduction and distribution, or selling or licensing copies, or posting to personal, institutional or third party websites are prohibited.

In most cases authors are permitted to post their version of the article (e.g. in Word or Tex form) to their personal website or institutional repository. Authors requiring further information regarding Elsevier's archiving and manuscript policies are encouraged to visit:

<http://www.elsevier.com/authorsrights>

Contents lists available at [SciVerse ScienceDirect](http://SciVerse.ScienceDirect.com)

Earth-Science Reviews

journal homepage: www.elsevier.com/locate/earscirev

Siberian Traps large igneous province: Evidence for two flood basalt pulses around the Permo-Triassic boundary and in the Middle Triassic, and contemporaneous granitic magmatism



Alexei V. Ivanov ^{a,*}, Huayiu He ^b, Liekun Yan ^b, Viktor V. Ryabov ^c, Artem Y. Shevko ^c, Stanislav V. Palesskii ^c, Irina V. Nikolaeva ^c

^a Institute of the Earth's Crust SB RAS, Irkutsk, Russia

^b Institute of Geology and Geophysics CAS, Beijing, China

^c Institute of Geology and Mineralogy SB RAS, Novosibirsk, Russia

ARTICLE INFO

Article history:

Received 4 February 2011

Accepted 2 April 2013

Available online 11 April 2013

Keywords:

⁴⁰Ar/³⁹Ar age

Large igneous provinces

Flood basalts

Siberian Traps

ABSTRACT

The Siberian Traps large igneous province is of enormous size ($\sim 7 \times 10^6 \text{ km}^2$) and volume ($\sim 4 \times 10^6 \text{ km}^3$). It contains effusive, intrusive and volcanoclastic rocks varying in compositions from ultramafic to felsic, though low-Ti basalts and their intrusive analogs are the predominant rock types. In this paper, we provide new ⁴⁰Ar/³⁹Ar ages for two lava units of the geographic center of the Siberian Traps, the Central Putorana region ($240.9 \pm 1.3/2.6/5.5$ and $246.6 \pm 1.4/2.7/5.6$ Ma, where ages are calculated relative to Bem4M with an assigned age of 18.7 (± 0.096) Ma and errors are stated in the form $\pm x/y/z$, where x and y and z are analytical, internal and external errors, respectively), three dolerite sills from the Angara-Taseevskaya syncline of the southeastern Siberian Traps ($242.8 \pm 1.3/2.6/5.0$ Ma, $239.1 \pm 1.1/2.5/4.9$ Ma and $255.8 \pm 4.7/5.3/6.9$ Ma) and a lamproite dyke from the Noril'sk region ($238.3 \pm 1.3/2.6/5.3$ Ma). In combination with available geochronologic data our results suggest that voluminous low-Ti basaltic magmatism appeared during different pulses. At least two volcanic pulses are recognized: at the Permo-Triassic boundary (~ 249 Ma or 252 Ma using the ⁴⁰Ar/³⁹Ar and U–Pb timescales, respectively) and about 10 Ma later in the Middle Triassic. Granitic magmatism overlapped in time with the two flood basalt pulses, but continued into the Late Triassic (~ 229 Ma using the U–Pb timescale). Prolonged magmatism of the Siberian Traps province is also supported by geologic observations and paleomagnetic data. New geochronologic findings are discussed in light of the different models for the origin of the Siberian Traps and applied to a Middle Triassic mass extinction event.

© 2013 Elsevier B.V. All rights reserved.

Contents

1. Introduction	59
2. Terminology: large igneous province and/or flood basalt province	60
3. Analytical procedure	60
4. Results for the Central Putorana and Noril'sk	61
4.1. Flood basalt stratigraphy and published geochronologic data	61
4.2. New ⁴⁰ Ar/ ³⁹ Ar dating results – lavas	61
4.3. New ⁴⁰ Ar/ ³⁹ Ar results – lamproite dyke	62
5. Results for the Angara-Taseevskaya syncline	64
5.1. Summary of previous studies	64
5.2. ⁴⁰ Ar/ ³⁹ Ar results – sills	65
6. Geologic evidence for long duration of the STLIP: Tunguska syncline example	65
7. Review of geochronologic and paleomagnetic data for the STLIP	66
7.1. ⁴⁰ Ar/ ³⁹ Ar ages	66
7.2. U–Pb ages	68
7.3. Paleomagnetic data	68

* Corresponding author. Tel.: +7 9149090363.
E-mail address: aivanov@crust.irk.ru (A.V. Ivanov).

8.	Duration of the Siberian Traps magmatism in comparison with other large igneous provinces	68
9.	Discussion	69
9.1.	Geodynamic implications	69
9.2.	Environmental impact	72
10.	Conclusions	74
	Acknowledgments	74
	Appendix A. Supplementary data	74
	References	74

1. Introduction

The Siberian Traps large igneous province is of enormous size ($\sim 7 \times 10^6 \text{ km}^2$) and volume ($\sim 4 \times 10^6 \text{ km}^3$) (Masaitis, 1983; Ivanov, 2007). It includes ultramafic alkaline, mafic and felsic rocks that erupted in different proportions within a vast region of several thousands of km^2 across Western and Eastern Siberia (Fig. 1). The Siberian Traps province is often considered to be of the very short duration of the basaltic volcanism, referred to as flood basalt volcanism. A large volume of lavas erupted at the Permo-Triassic boundary within probably less than 1 Ma in the northern part of the Siberian Traps province. Near Noril'sk the lavas reach thicknesses of over 3 km and further to the northeast, in the Maimecha-Kotui region, half of the total lava pile is composed of ultramafic rocks (meimechites) (Renne and Basu, 1991; Basu et al., 1995; Venkatesan et al., 1997; Kamo et al., 2003; Reichow et al., 2009) (Fig. 1). Volcanic rocks of this age were met in drillcore in the West Siberian Basin (Reichow et al., 2002, 2009) (Fig. 1). This Permo-Triassic volcanic pulse is known as Siberian flood basalt volcanism. However, older and younger $^{40}\text{Ar}/^{39}\text{Ar}$ ages have been reported for dolerite intrusions and basaltic lava (Baksi and Farrar, 1991; Dalrymple et al., 1995; Reichow et al., 2002; Vrublevskii et al., 2004; Ivanov et al., 2005; Walderhaug et al., 2005; Ivanov et al., 2009; Reichow et al., 2009). The reliability of these $^{40}\text{Ar}/^{39}\text{Ar}$ ages was debated (e.g. Baksi, 2007a,b). It is now accepted that at least some of the

published ages are anomalously old due to the presence of excess ^{40}Ar (see Renne, 1995 for reconsideration of $^{40}\text{Ar}/^{39}\text{Ar}$ biotite age from Noril'sk-I intrusion), while some of the ages could be anomalously young due to partial loss of radiogenic ^{40}Ar (Baksi, 2007a,b). Nonetheless, Triassic ages from some regions, for example the Angara-Taseevskaya syncline in the southeastern part of the province (Ivanov et al., 2005, 2009), and the Chelyabinsk basin (Reichow et al., 2009) in the western part of the province (Fig. 1), are not questioned. Thus, it is timely to consider Siberian Traps magmatism beyond the well-defined Permo-Triassic flood basalt event.

In addition to basalts, anorogenic granites are abundant in the peripheral parts of the Siberian Traps province and are considered to be related to basaltic magmatism (Vernikovskiy et al., 2003; Dobretsov et al., 2005). U–Pb dating suggests that granitic magmatism started contemporaneously with basaltic magmatism and lasted into the Triassic (Vladimirov et al., 2001; Kamo et al., 2003; Vernikovskiy et al., 2003; Vernikovskaya et al., 2010). Thus, further questions concerning the timing and distribution of both basaltic and granitic magmatism should be answered.

In this paper we report $^{40}\text{Ar}/^{39}\text{Ar}$ ages from two samples collected from the previously undated Central Putorana region, near the geographic center of the Siberian Traps, from three samples from the Angara-Taseevskaya syncline, known previously for the existence of both Permo-Triassic and Triassic magmatism (Ivanov et al., 2005,

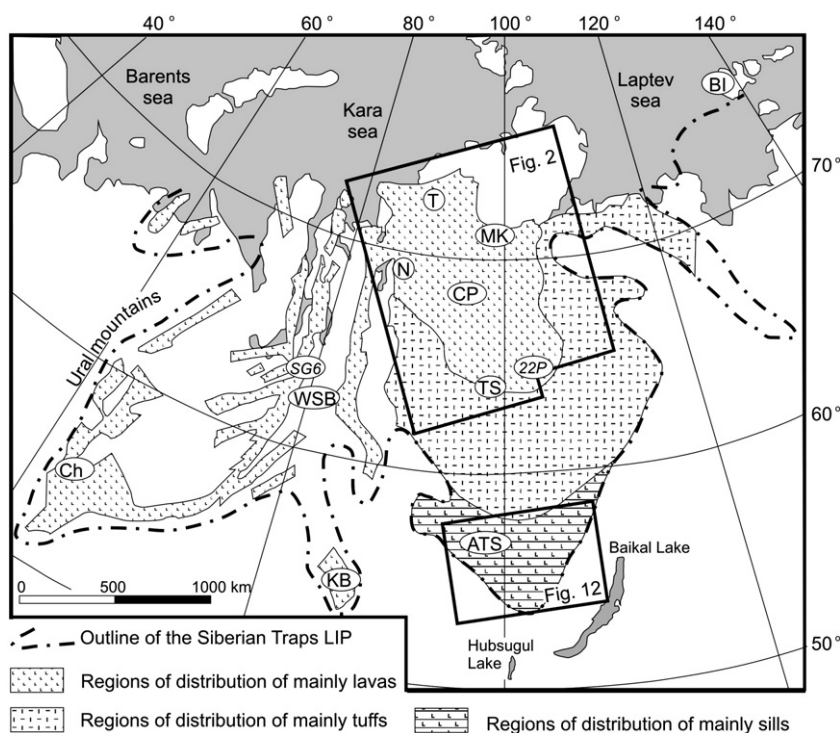


Fig. 1. General map of the Siberian Traps large igneous province (simplified and modified after Masaitis, 1983). Localities mentioned in the text: N – Noril'sk, T – Taimyr peninsula, MK – Maimecha-Kotui area, CP – Central Putorana, TS – Tunguska syncline, ATS – Angara-Taseevskaya syncline, KB – Kuznetsk Basin, Ch – Chelyabinsk, BI – Belkov island, WSB – West Siberian Basin, SG6 – super deep drill-hole no. 6, 22P – regional drill-hole no. 22.

2009; Paton et al., 2010), and from one sample of a lamproite dyke from Noril'sk, a classic locality for voluminous Permo-Triassic flood basalt volcanism. We also review available geochronologic ($^{40}\text{Ar}/^{39}\text{Ar}$ and U–Pb) and paleomagnetic data from other regions to show that the Siberian Traps magmatism lasted for about 25–30 Ma, and discuss our results in terms of different models for the origin of the Siberian Traps province and their application for the study of mass extinctions.

2. Terminology: large igneous province and/or flood basalt province

Recently, Sheth (2007) and Bryan and Ernst (2008) addressed the definition and terminology of large igneous provinces and their relation to flood basalt provinces. A flood basalt province is a region covered by thick units of basaltic lava. "Basaltic" is used in a broad sense including both silica undersaturated and oversaturated rocks such as meimechites and basaltic andesites, respectively, in addition to classic basalts. It is known that enormous amounts of basaltic magma can be erupted during geologically short periods (<1 Ma), and the Siberian Traps province is no exception (Renne and Basu, 1991; Kamo et al., 2003; Reichow et al., 2009). In this sense, the Siberian Traps is a flood basalt province. However, traditionally various rock types were considered as constituent parts of the Siberian Traps. For example, the Bolgokhtokh massif of granites and related rocks is spatially closely associated with the famous flood basalt units of nearby Noril'sk (Komarova, 1968). These granites were assumed to be differentiates of basaltic magma (Ryabov et al., 2001, in press). It appeared that the age of the Bolgokhtokh granites is significantly (>20 Ma) younger than that of the neighboring flood basalts (Dalrymple et al., 1995; Kamo et al., 2003), but granites similar in composition are known from the Taimyr and Kuznetsk Basins where they were emplaced contemporaneously with the flood basalts (Vladimirov et al., 2001; Vernikovskiy et al., 2003). Coeval granites and basalts are also known in other peripheral regions of the Siberian Traps (Dobretsov et al., 2005).

3. Analytical procedure

The analytical procedures were essentially the same as in our previous study (Ivanov et al., 2009). Briefly, major and trace elements (the latter including platinum group elements (PGE)) were determined by classic wet chemistry at the Institute of the Earth's Crust SB RAS (Irkutsk, Russia) and by inductively-coupled plasma mass-spectrometry at the Institute of Geology and Mineralogy SB RAS (Novosibirsk, Russia), respectively. PGE concentrations were determined by isotope dilution modified after Pearson and Woodland (2000). Analytical protocols for the trace element and PGE analyses have been described elsewhere (Nikolaeva et al., 2008; Palesskii et al., 2009). Measured concentrations are listed in Table 1.

As for $^{40}\text{Ar}/^{39}\text{Ar}$ dating, two samples (XA39 and XZ1) from the Central Putorana region were processed in exactly the same way as samples from our previous study (Ivanov et al., 2009). The samples selected for $^{40}\text{Ar}/^{39}\text{Ar}$ dating were the least altered in the available collection. Secondary alteration was assessed on the basis of petrographic investigation under a polarizing microscope and based on loss on ignition values (LOI) (Table 1). The samples were crushed and sieved, and plagioclase crystals were then picked under a binocular microscope. The plagioclase separates were pretreated by diluted HF to remove ingrowths of secondary minerals if such plagioclases were not recognized under binocular. Irradiation parameters and the stepwise-heating procedure are listed in He et al. (2004) and Ivanov et al. (2009). The mineral standard used for the age calculations was Bern4M with an assigned age of 18.7 (± 0.096) Ma, which corresponds to the age of 98.79 Ma for standard GA1550 (Baksi et al., 1996; Renne et al., 1998). Ages were calculated using the decay constants of Steiger and Jäger (1977). Discussing the $^{40}\text{Ar}/^{39}\text{Ar}$

Table 1
Major and trace element data for samples dated in this work.

	XZ1	XA39	ZP10	ST-05-34	ST-05-4	ST-05-48
SiO ₂	50.64	49.64	53.78	49.44	48.73	47.94
TiO ₂	0.95	1.30	1.62	1.50	2.13	1.93
Al ₂ O ₃	15.78	15.41	8.85	13.60	14.70	14.00
Fe ₂ O ₃	3.63	2.69	4.75	3.27	5.33	3.78
FeO	6.62	9.18	2.54	9.30	8.78	10.00
MnO	0.14	0.17	0.05	0.20	0.17	0.26
MgO	6.17	6.17	7.76	6.41	5.05	5.55
CaO	10.29	10.35	5.21	11.70	10.00	10.32
Na ₂ O	2.44	2.30	1.06	2.28	2.74	3.12
K ₂ O	0.91	0.31	8.3	0.58	0.69	0.86
P ₂ O ₅	0.20	0.14	2.13	0.15	0.25	0.19
LOI	2.15	1.96	3.48	2.00	1.63	1.79
Total	99.92	99.62	99.63	100.43	100.20	99.74
Sc	45	51	24			
V	256	338	128			
Cr	152	159	324			
Co	41	52	24			
Ni	62	88	72			
Rb	17.6	5.1	181	11.4		
Sr	380	255	3464	183		
Y	34	31	35	29		
Zr	133	103	647	108		
Nb	8.8	5.1	64	5.5		
Cs	2.5	0.42	0.44	0.45		
Ba	408	165	7130	172		
La	18.8	8.2	129	9.5		
Ce	36	17.6	242	22		
Pr	4.8	2.7	34	3.3		
Nd	20.0	12.6	134	12.5		
Sm	4.3	3.6	21	3.2		
Eu	1.17	1.19	5.4	1.23		
Gd	4.4	4.2	13.8	4.7		
Tb	0.72	0.75	1.56	0.75		
Dy	4.8	4.7	7.0	5.4		
Ho	1.05	1.01	1.12	1.02		
Er	3.1	2.9	2.8	3.0		
Tm	0.47	0.45	0.35	0.46		
Yb	3.2	2.8	2.2	3.1		
Lu	0.46	0.40	0.30	0.50		
Hf	3.2	2.7	18.0	3.3		
Ta	0.50	0.35	2.7	0.36		
Pb	6.6	4.0	66			
Th	2.1	1.09	13.2	1.52		
U	1.06	0.54	4.4	0.36		
Ru	0.66	0.34	0.02			
Pd	1.85	15.1	b.d.l.			
Ir	0.11	0.09	4.35			
Pt	1.39	15.6	10.15			

Note: Major elements – wt.%, all trace elements from Sc to U – ppm, PGE – ppb. B.d.l. – below detection limit. Empty cells – not analyzed.

analytical data we use the following terms: plateau, isochron/errorchron (isotope correlation) and integrated step ages. 'Plateau' is defined for a number of consecutive steps that together comprise more than 50% of the ^{39}Ar released and in which the apparent ages belong to the same normal distribution at 95% confidence level according to the chi-square test (Baksi, 2007a; <http://www.mantleplumes.org/ArAr.html>). For this, the calculated mean square weighted deviation value (MSWD) was multiplied by the corresponding degree of freedom (i.e. number of steps minus 1 for a plateau, and number of steps minus 2 for an isotope correlation) and thus the obtained chi-square value was compared with available chi-square tables (e.g., Müller et al., 1979). If consecutive steps do not pass the chi-square test, we refer to it as 'integrated step' age. 'Isochrons' and 'errorchrons' are also calculated in $^{40}\text{Ar}/^{36}\text{Ar}$ – $^{40}\text{Ar}/^{39}\text{Ar}$ coordinates and distinguished on the basis of a chi-square test. Errors are stated in the form $\pm x$ or $\pm x/y$ or $\pm x/y/z$, where x, y and z are analytical, internal and external errors, respectively (Koppers, 2002). The analytical error does not include the error of the age standards, whereas the internal error does. The former is used to compare ages obtained for samples

of the same irradiation. The latter error is used for comparing ages obtained from different irradiations. External errors account for ^{40}K decay uncertainties (Koppers, 2002). Complete analytical tables are available as supplementary material.

Three further samples (ST-05-4, ST-05-34, ST-05-48) from the Angara-Taseevskaya syncline were processed in exactly the same way as samples XA39 and XZ1, except that they were pre-treated with HNO_3 instead of HF. The standard for the age calculations was TCs with an assigned age of $28.34 (\pm 0.085)$ Ma, which corresponds to the age of 98.79 Ma for standard GA1550 (Renne et al., 1998).

One sample of a lamproite dyke (ZP10) from Noril'sk was analyzed at the Institute of Geology and Geophysics CAS (Beijing, China) and at the Institute of the Earth's Crust SB RAS (Irkutsk, Russia). Mica crystals were picked for $^{40}\text{Ar}/^{39}\text{Ar}$ dating. The aliquot analyzed at the Institute of Geology and Geophysics CAS (Beijing, China) was pre-treated with HF, while two other aliquots analyzed at the Institute of the Earth's Crust SB RAS (Irkutsk, Russia) were not treated by any acids. Measurements were performed on a MM5400 mass-spectrometer at the former institute and on an Argus VI mass-spectrometer at the latter. The mineral standard used for the age calculations in both cases was Bern4M (see above information on the age of the standard). Irradiation parameters used at the Institute of the Earth's Crust SB RAS (Irkutsk, Russia) were the same as in other $^{40}\text{Ar}/^{39}\text{Ar}$ studies delivered from the Institute of Geology and Mineralogy SB RAS (Novosibirsk, Russia) (e.g. Vernikovskiy et al., 2003; Travin et al., 2009).

4. Results for the Central Putorana and Noril'sk

4.1. Flood basalt stratigraphy and published geochronologic data

The northern part of the Siberian flood basalt province was subdivided into different regions with their own stratigraphy (Zolotuhin et al., 1986) (Fig. 2). Each such region is characterized by petrographically and chemically distinct stratigraphic units, referred to as suites (Fig. 3). Lacking precise radioisotopic dating, the general strategy for the correlation of suites between different regions was based on the assumption that petrographically and chemically similar lava suites have the same age. Within the Noril'sk-Kharaelakh and Khantaisk-Rybninsk regions, the Nadezhdinsky suite was traced in natural outcrops and by drilling. The thickness of the Nadezhdinsky suite in these regions varies from 200 to 570 m (Zolotuhin et al., 1986). In the Russian geologic literature, volcanic deposits below the Nadezhdinsky suite with maximal thicknesses of 1 km are referred to as basalts of the 'rift stage', and those above the Nadezhdinsky suite with maximal thicknesses of up to 2.5 km are referred to as basalts of the 'flood stage' (e.g. Al'mukhamedov et al., 2004). In the Noril'sk-Kharaelakh and Kamensk regions, an unconformity was mapped between the Nadezhdinsky and Morongovskiy suites; in the Khantaisk-Rybninsk region the unconformity was mapped between the Nadezhdinsky and Ayansky and between the Ayansky and Honno-Makitsky suites, whereas in the Central Putorana region the unconformity was mapped between the Ayansky and Honno-Makitsky suites (Fig. 4). Generally speaking, the majority of rocks below the Nadezhdinsky suite belong to a high-Ti rock series, whereas almost all rocks above the Nadezhdinsky suite are classified as low-Ti basalts, also known in the literature as low-K tholeiites (Fedorenko et al., 1996; Al'mukhamedov et al., 2004). Basalts of the Nadezhdinsky suite belong to a particular sub-type of the low-Ti rock series (Fedorenko et al., 1996).

$^{40}\text{Ar}/^{39}\text{Ar}$ ages available for those suites from which samples were previously dated were recalculated to the same age standard and are shown in Fig. 3. Two things are seen immediately in Fig. 3. First, the $^{40}\text{Ar}/^{39}\text{Ar}$ ages obtained by different studies for the same suites in the closely spaced Noril'sk-Kharaelakh and Khantaisk-Rybninsk regions are in good agreement. Secondly, there is significant disagreement between ages for the Tunguska region obtained by Baksi and Farrar (1991) and for south Central Putorana region by Reichow et al. (2009).

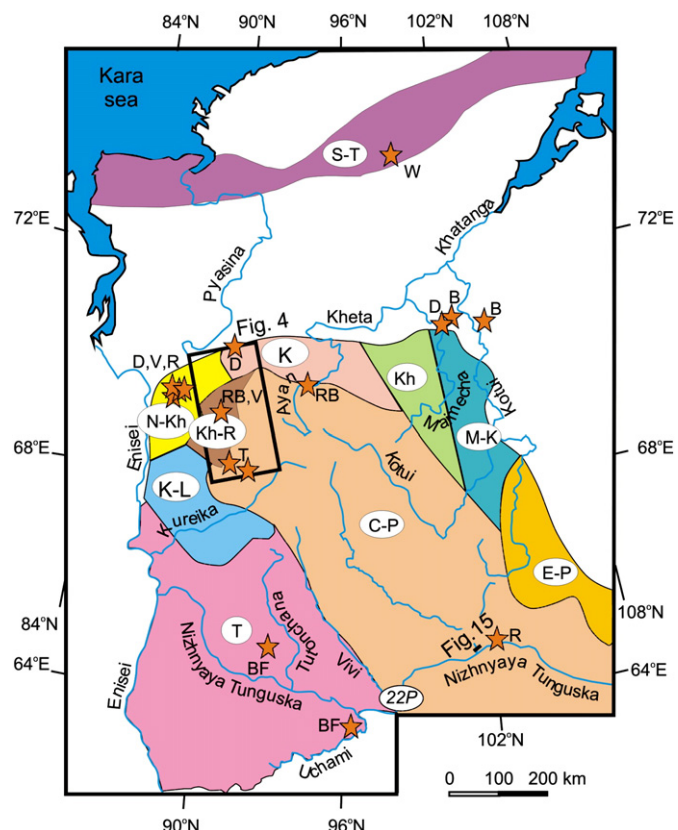


Fig. 2. Permo-Triassic magmatic regions of the northern part of the Siberian Traps large igneous province (after Zolotuhin et al., 1986). Volcanic regions are shown in different colors: N-Kh – Noril'sk-Kharaelakh, Kh-R – Khantaisk-Rybninsk; K – Kamensk; Kh – Kheta; M-K – Maimecha-Kotui; K-L – Kureika-Letninsk; C-P – Central Putorana; E-P – Eastern Putorana; T – Tunguska; S-T – South Taimyr. Stars mark localities of samples dated by $^{40}\text{Ar}/^{39}\text{Ar}$: BF – Baksi and Farrar, 1991; RB – Renne and Basu, 1991; D – Dalrymple et al., 1995; B – Basu et al., 1995; V – Venkatesan et al., 1997; W – Walderhaug et al., 2005; R – Reichow et al., 2009; T – this work. U–Pb ages of Kamo et al. (2003) are from the Noril'sk-Kharaelakh and Maimecha-Kotui volcanic regions. Location of drill-hole no. 22P is also shown. (For interpretation of the references to color in this figure legend, the reader is referred to the web version of this article.)

The samples from these two studies were collected from widely separated localities.

Most of the $^{40}\text{Ar}/^{39}\text{Ar}$ ages scatter around 249 Ma (Fig. 3), in general agreement with U–Pb data obtained for lavas and intrusions from the same regions (Kamo et al., 2003), after the systematic difference between $^{40}\text{Ar}/^{39}\text{Ar}$ and U–Pb ages is accounted for (Min et al., 2000; Ivanov, 2006).

4.2. New $^{40}\text{Ar}/^{39}\text{Ar}$ dating results – lavas

For our $^{40}\text{Ar}/^{39}\text{Ar}$ study, we have taken a low-Ti basalt sample (XA39) from the previously undated Honno-Makitsky suite at the southern shore of Lake Khantaiskoe (Fig. 4). Here, the Honno-Makitsky suite is underlain by a 45 m thick tuff layer with numerous plant impressions. The Honno-Makitsky suite was considered an analog of the Mokulaevskiy suite of the Noril'sk-Kharaelakh and Khantaisk-Rybninsk regions (Fig. 3). It is shown in Figs. 5 and 6 that sample XA39 has very similar trace and platinum group element abundances as samples from the Mokulaevskiy suite. The only differences are higher Pb and lower Ir concentrations in XA39. Other elements have similar concentrations and, hence, similar normalized element patterns; thus, we consider the Honno-Makitsky and Mokulaevskiy suites as geochemical analogs. In other words, from a geochemical point of view the dated sample XA39 belongs to the low-Ti rock series of the so-called flood stage of the Siberian Traps. However, $^{40}\text{Ar}/^{39}\text{Ar}$ dating of sample XA39 has shown that

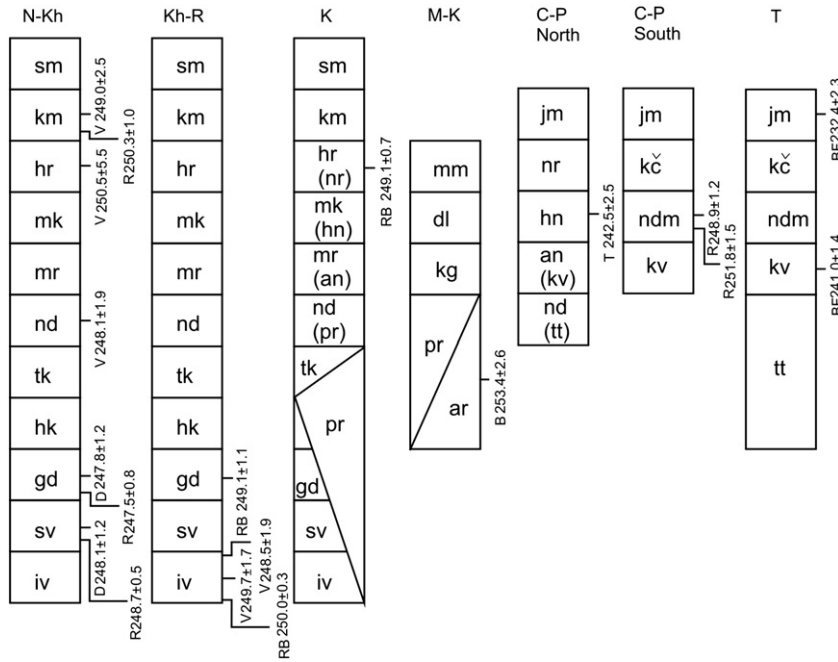


Fig. 3. Stratigraphic subdivisions within different volcanic regions of the Siberian Traps large igneous province (after Zolotuhin et al., 1986 with modifications). Stratigraphic subdivisions (suites): iv – Ivakinsky; sv – Syverminsky; gd – Gudchikhinsky; hk – Khakanchansky; tk – Tuklonsky; nd – Nadezhdinsky; mr – Morongovsky; mk – Mokulaevsky; hr – Kharaelakhsky; km – Kunginsky; sm – Samoedsky; pr – Pravoboyarsky; an – Ayansky; hn – Honna-Makitsky; nr – Nerakarsky; ar – Arydzhansky; kg – Kogotsky; dl – Delkansky; mm – Maimechinsky; tt – Tutonchansky; kv – Korvuchansky; ndm – Nidymsky; kč – Kochechumsky; jm – Jambukansky. $^{40}\text{Ar}/^{39}\text{Ar}$ ages in Ma are shown close to the dated suites. The ages are recalculated from published studies relative to a K-Ar age of 98.79 Ma for the standard GA1550 (Renne et al., 1998). Abbreviations for the volcanic regions: N-Kh – Noril'sk-Kharaelakh, Kh-R – Khantaisk-Rybninsk; K – Kamensk; M-K – Maimecha-Kotui; C-P – Central Putorana; T – Tunguska. Abbreviations for the $^{40}\text{Ar}/^{39}\text{Ar}$ ages: BF – Baksi and Farrar, 1991; RB – Renne and Basu, 1991; D – Dalrymple et al., 1995; B – Basu et al., 1995; V – Venkatesan et al., 1997; W – Walderhaug et al., 2005; R – Reichow et al., 2009; T – this work.

the Honna-Makitsky suite is significantly (~8 Ma) younger than the Mokulaevsky suite. Sample XA39 yielded a well-defined plateau age of $240.9 \pm 1.3/2.6$ Ma (Fig. 7). The K/Ca ratios of the plateau steps are relatively uniform (Fig. 7) and suggest that the age-constraining mineral is plagioclase of bytownite composition. The plateau steps define a $242.5 \pm 2.1/3.1$ Ma isochron age with an atmospheric initial $^{40}\text{Ar}/^{36}\text{Ar}$ value (Fig. 7, Table 2).

Low-Ti basalt sample XZ1 from the Nadezhdinsky suite was collected at the northern shore of Lake Khantaiskoe (Fig. 4). As shown in Figs. 5 and 6, XZ1 has trace element and PGE patterns very similar to samples from the Nadezhdinsky suite in the Noril'sk-Kharaelakh and Khantaisk-Rybninsk regions, with the exception of higher Ir, Ru and Rb abundances. Rubidium is a mobile element and may be redistributed during secondary alteration, which is significant for the majority of samples used in previous studies (Wooden et al., 1993; Al'mukhamedov et al., 2004). The different Ir and Ru abundances could be due to analytical limitations for determining the concentrations of these elements at extremely low concentrations (Table 1). Alternatively, the differences may be due to the natural variability of these elements in different samples of the same lava suite.

Sample XZ1 did not yield statistically meaningful plateau and isochron ages (Fig. 7). The specific pattern in which the apparent ages decrease from low to high temperature steps, flattening at the intermediate temperature steps, is probably due to recoil of ^{39}Ar (Foland and Xu, 1990). Five steps in the middle of the age spectrum have an integrated age of $246.6 \pm 1.4/2.7$ Ma, which overlaps within internal error with the 248.1 ± 1.9 Ma age (of the Nadezhdinsky suite) published by Venkatesan et al. (1997) (the reported error in this study is analytical). K/Ca ratios for the integrated steps of XZ1 are about 3 times higher than for the plateau-defining steps of XA39, which is in agreement with the 3 times higher potassium content of XZ1 compared to XA39 (Table 1). The errorchron age for the same five

integrated steps of sample XZ1 is $248.7 \pm 3.0/3.8$ Ma, with an atmospheric initial $^{40}\text{Ar}/^{36}\text{Ar}$ ratio (Fig. 7, Table 2).

Irrespective of problems associated with ^{39}Ar recoil, the sample XZ1 yields an age that is in agreement with that of a previous $^{40}\text{Ar}/^{39}\text{Ar}$ study (Venkatesan et al., 1997). The age of the Nadezhdinsky suite in the Noril'sk-Kharaelakh and Central Putorana regions overlaps with the ~249 Ma age (according to the $^{40}\text{Ar}/^{39}\text{Ar}$ timescale) for the major peak of the Siberian flood basalts (Renne and Basu, 1991; Basu et al., 1995; Venkatesan et al., 1997; Reichow et al., 2002, 2009). In contrast, the sample XA39 from the Honna-Makitsky suite from the Central Putorana region yielded statistically meaningful plateau and isochron ages, which are about 8 Ma younger compared to the major peak of the Siberian flood basalts. The time gap between formation of the Nadezhdinsky and Honno-Makitsky suites does not contradict field data, because the observed unconformity marked by the tuff layer at the base of the Honno-Makitsky suite testifies of a gap in volcanism.

Despite the younger age of the Honna-Makitsky suite, the lava of this suite has a geochemistry typical of Siberian flood basalts. Considering the size of the Central Putorana region (~ 3×10^5 km², Fig. 2), and the cumulative thickness of the Honna-Makitsky, Nerakarsky and Jambukansky suites (600–1250 m, Zolotuhin et al., 1986), the volume of the lava erupted during this younger pulse of volcanism is about $1.8\text{--}3.75 \times 10^5$ km³. Sheth (2007) and Bryan and Ernst (2008) suggest minimum volumes of 0.5×10^5 km³ and 1×10^5 km³, respectively, for a large igneous province. The volume of the younger suites of the Central Putorana region exceeds both these minimum values. Thus, the obtained ages suggest that, in addition to the well-known Permo-Triassic pulse of the Siberian flood basalts, we dated a Middle Triassic pulse of flood basalts.

4.3. New $^{40}\text{Ar}/^{39}\text{Ar}$ results – lamproite dyke

In addition to thick lava units (Fig. 3), the Noril'sk region is known for sills and dykes, a majority of which are basaltic in composition.

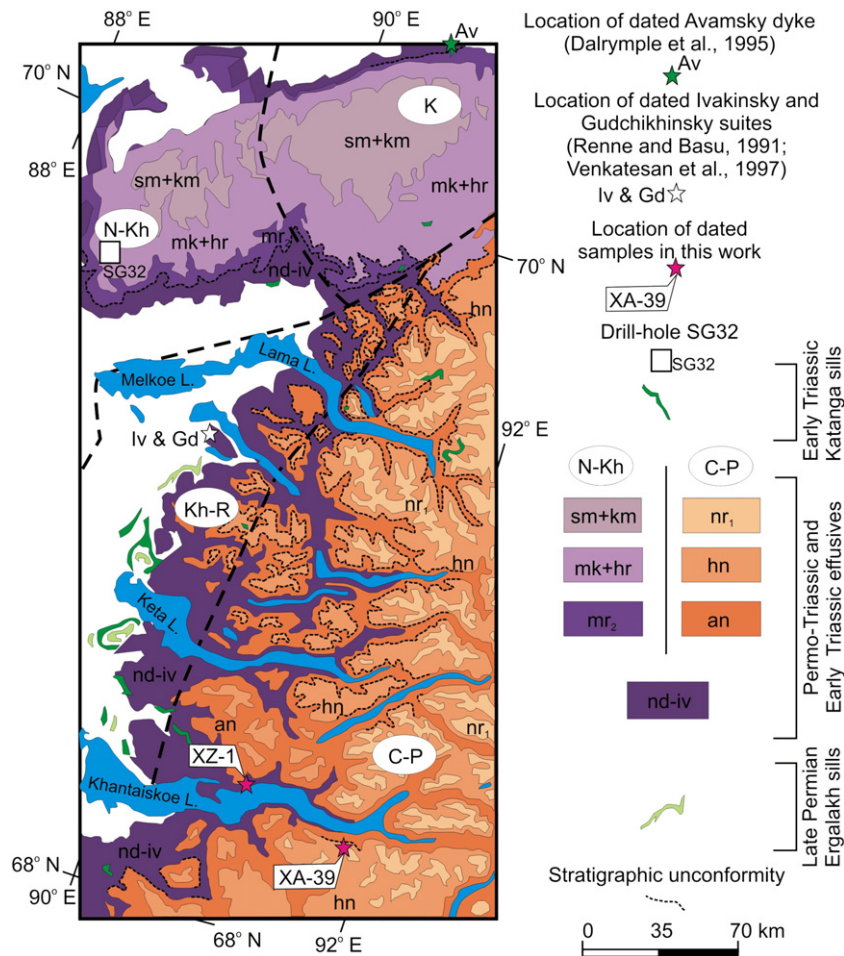


Fig. 4. Geologic map of Late Permian and Early Triassic magmatic rocks at the junction of the Noril'sk-Kharaelakh, Khantaisk-Rybninsk, Kamensk and Central Putorana volcanic regions (partly after Malitch, 1999, with modifications of color pattern). Stratigraphic unconformities are shown as dotted lines following Geologic Survey map data and from authors' field observations, e.g. Ryabov et al., 2001, in press). Volcanic regions are separated by thick dashed lines (after Zolotuhin et al., 1986). Abbreviations for the provinces and suites are the same as in Fig. 2. In a recent study by Reichow et al. (2009) samples for $^{40}\text{Ar}/^{39}\text{Ar}$ dating were collected from the SG32 drill-hole.

However, dykes of more exotic compositions are also present, such as rare lamproite dykes. These were previously named as lamprophyres, however, in terms of their chemistry, they fall into the field of lamproites. They are characterized by molar ratios $\text{Na}_2\text{O}/\text{K}_2\text{O} > 3$, $\text{K}_2\text{O}/\text{Al}_2\text{O}_3 > 0.8$, $(\text{K}_2\text{O} + \text{Na}_2\text{O})/\text{Al}_2\text{O}_3 > 1$, $\text{FeO} < 10$ wt.%, $\text{CaO} < 10$ wt.%, TiO_2 1–7 wt.%, $\text{Ba} > 5000$ ppm, $\text{Zr} > 500$ ppm, $\text{Sr} > 1000$ and $\text{La} > 200$ (Wooley et al., 1996). By all these chemical indexes (except La) sample ZP10 is a lamproite (Table 1), and, because phlogopite crystals appear as phenocrysts (Fig. 8), it should be named a phlogopite lamproite.

The lamproite dyke from which the sample ZP10 was taken cuts through lower lava units of the Ivakinsky, Tuklonsky and Nadezhdinsky suites. The relationship with upper lava units was not observed in the field. The lamproite is highly enriched compared to any lava in the Noril'sk region and is similar to phlogopite lamproites from classic locality in the Leucite Hills of Wyoming, USA, with the exception of Hf and heavy rare earth elements (Fig. 9).

Fig. 10 shows $^{40}\text{Ar}/^{39}\text{Ar}$ dating results obtained at the Institute of Geology and Geophysics CAS (Beijing, China) for a phlogopite separate

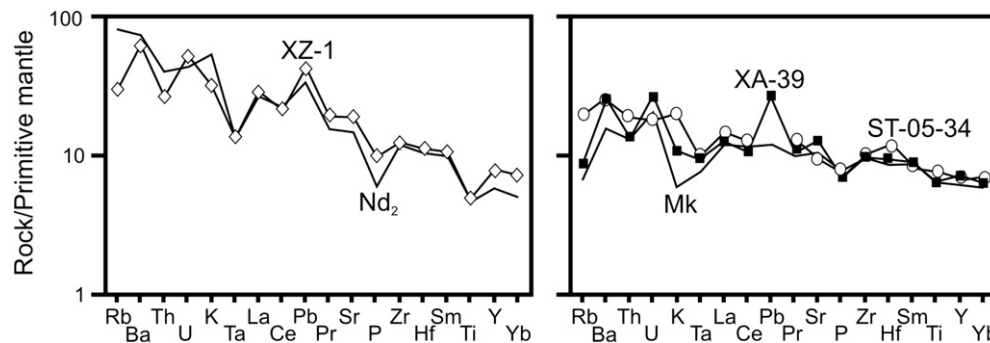


Fig. 5. Comparison of trace element patterns of samples XZ-1 (white diamonds), XA-39 (black squares) and ST-05-34 (open circles), together with averages of the Nadezhdinsky – 2 sub-suite (Nd_2) and Mokulaevsky suite (Mk) of the Noril'sk-Kharaelakh volcanic region (averages were calculated from the data of Wooden et al., 1993; Al'mukhamedov et al., 2004; most of the samples from these studies are from the SG32 drill-hole (see Fig. 4)). Trace element abundances are normalized to the primitive mantle composition of McDonough and Sun (1995).

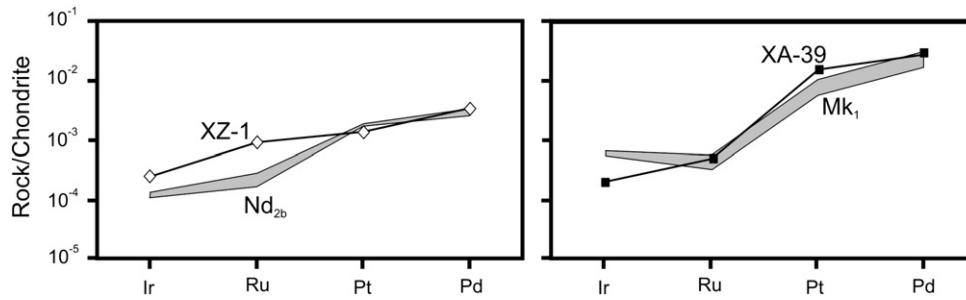


Fig. 6. Comparison of PGE patterns in samples XZ-1 (white diamonds) and XA-39 (black squares) with the range of concentrations of the Nadezhdinsky – 2b sub-suite (Nd_{2b}) and Mokulaevsky – 1 sub-suite (Mk₁) of the Noril'sk-Kharaelakh region. The data for the Noril'sk-Kharaelakh region are from Lightfoot and Keays (2005). All but one sample of Lightfoot and Keays (2005) are from the SG32 drill-hole (see Fig. 4). PGE abundances are normalized to chondrite composition of McDonough and Sun (1995).

treated by HF from the lamproite sample ZP10. Five steps of the sample ZP10 form a well-defined plateau age of $238.3 \pm 0.8/2.4$ Ma, which is concordant with isochron age calculated for the same steps (Fig. 10, Table 2). Fig. 11 shows $^{40}\text{Ar}/^{39}\text{Ar}$ age spectra for two aliquots of the same phlogopite sample analyzed at the Institute of the Earth's Crust SB RAS (Irkutsk, Russia). Both aliquots yielded well-defined plateau ages of $235.5 \pm 0.5/1.2$ Ma and $235.3 \pm 0.8/1.5$ Ma, which are slightly younger compared to the plateau age obtained at the Institute of Geology and Geophysics CAS (Beijing, China) on the basis of analytical errors, but overlap on the basis of internal error. Ages obtained in both laboratories show that the lamproite dyke was emplaced in the

Middle Triassic. For further consideration we leave the age obtained at the Institute of Geology and Geophysics CAS (Beijing, China).

5. Results for the Angara-Taseevskaya syncline

5.1. Summary of previous studies

In the Angara-Taseevskaya syncline the following large dolerite sills were identified: Usol'skii and Zayarskii (probably connected at depth), Tulunskii, Padunskii, Chuna-Biryusinskii and Tolstomysovskii (Feoktistov, 1978) (Fig. 12). In previous studies all samples dated by

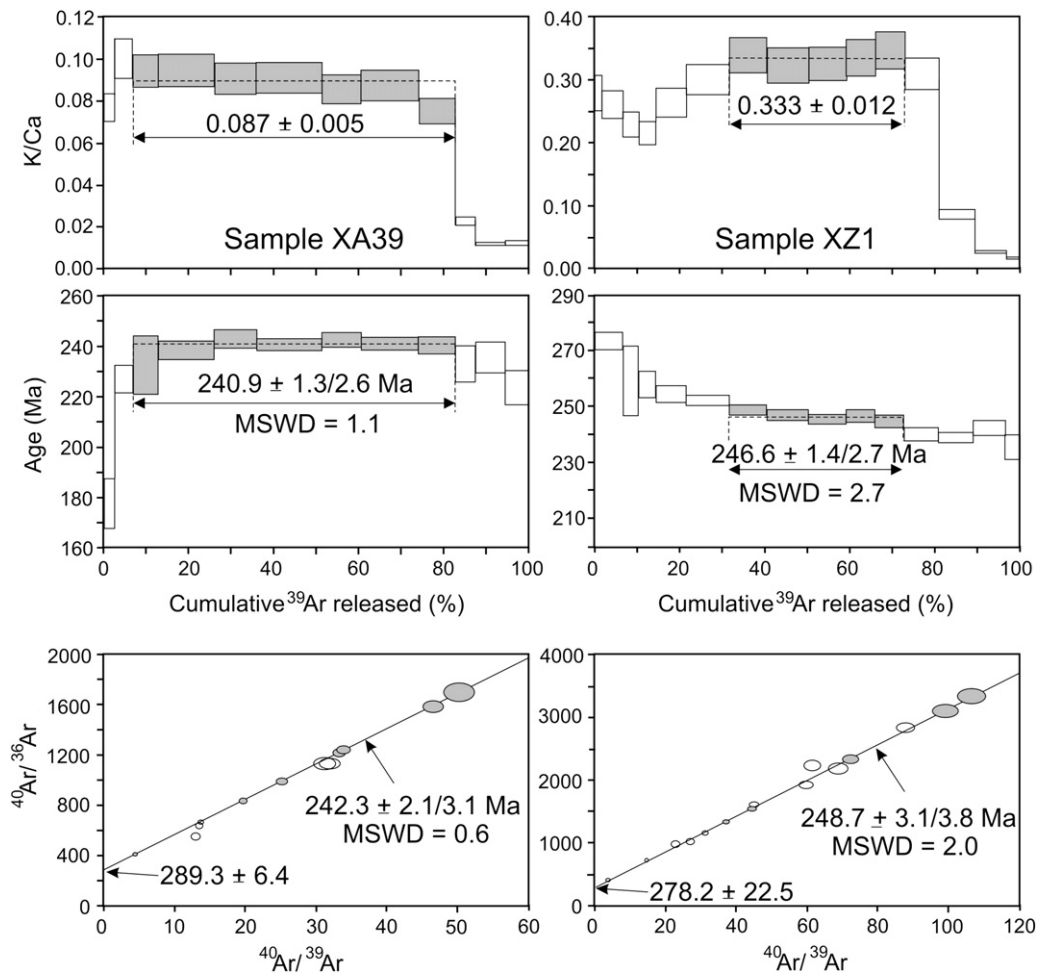


Fig. 7. Stepwise heating argon release spectra and isochrons for plagioclase separates of basaltic samples XA39 and XZ1. Error bars in the diagrams are analytical at the 2-sigma level. Steps used for calculations of plateau and isochron ages are shown in gray. Sample XA39 passes the chi-square test for c and isochron ages, whereas sample XZ1 does not.

Table 2
Summary of $^{40}\text{Ar}/^{39}\text{Ar}$ data.

Sample	'Plateau' or 'integrated steps'			'Isochron' or 'errorchron'		Total fusion age (Ma)
	^{39}Ar (%)	Age (Ma)	K/Ca	Age (Ma)	$^{40}\text{Ar}/^{36}\text{Ar}_0$	
XA39	75.8 (7)	240.9 ± 1.3/2.6/5.5 (P)	0.087 ± 0.005	242.5 ± 2.1/3.1/5.7 (I)	289.3 ± 6.4	236.3 ± 1.3/2.6/5.4
XZ1	41.2 (5)	246.6 ± 1.4/2.7/5.6 (IS)	0.333 ± 0.012	248.6 ± 3.1/3.8/6.3 (E)	278.3 ± 22.6	248.3 ± 0.8/2.5/5.5
ZP10	71.6 (5)	238.3 ± 1.3/2.6/5.3 (P)	6.172 ± 1.547	238.3 ± 2.3/3.2/5.7 (I)	311.7 ± 314.6	237.0 ± 2.0/3.0/5.6
ST-05-4	53.3 (5)	242.8 ± 1.3/2.6/5.0 (P)	0.412 ± 0.078	244.3 ± 2.9/3.7/5.7 (I)	279.5 ± 27.9	220.3 ± 6.8/7.1/8.1
ST-05-48	89.7 (10)	239.1 ± 1.1/2.5/4.9 (P)	0.185 ± 0.028	238.0 ± 2.0/3.0/5.1 (I)	301.6 ± 9.9	241.1 ± 2.4/3.3/5.3
ST-05-34	51.7 (5)	255.8 ± 4.7/5.3/6.9 (P)	0.045 ± 0.005	260.4 ± 12.7/12.9/13.7 (I)	289.8 ± 14.6	257.3 ± 9.5/9.8/10.8

Figures in parentheses represent the number of steps used for calculation. 'Isochrons' were calculated on the same steps as 'plateau' and 'integrated step' ages. Errors are at the 2 sigma level, shown as x/y/z for analytical, internal and external errors, respectively (Koppers, 2002). Preferred ages are shown in bold. Ages in italic are informative only. P, IS, I, and E are acronyms for 'plateau', 'integrated steps', 'isochron' and 'errorchron', respectively.

the $^{40}\text{Ar}/^{39}\text{Ar}$ method yielded Triassic ages (about 244 Ma, Ivanov et al., 2005; about 240 Ma, Ivanov et al., 2009). However, U–Pb dating yielded older ages (250–254 Ma) (Svensen et al., 2009; Paton et al., 2010). Samples dated by U–Pb and $^{40}\text{Ar}/^{39}\text{Ar}$ methods were collected from different regions separated more than 100 km from each other (Fig. 12).

For this study, we collected additional samples and sampling had taken place before the U–Pb dating results became known. In total 8 samples were taken of which only three (ST-05-4, ST-05-34, ST-05-48) yielded plateau ages that passed the chi-square test. Trace and platinum group element abundances are not yet available for all these samples, but petrographically they are not different from the samples studied by Ivanov et al. (2009), and resemble low-Ti basalts of the Mokulaevsky suite of the Noril'sk-Kharaelakh region (Ivanov et al., 2008, 2009) (Fig. 5).

5.2. $^{40}\text{Ar}/^{39}\text{Ar}$ results — sills

Fig. 13 shows the $^{40}\text{Ar}/^{39}\text{Ar}$ results for samples ST-05-4 and ST-05-48 from the Tulunskii sill and Padunskii sill, respectively. Both samples yielded plateau ages of $242.8 \pm 1.3/2.6$ Ma and $239.1 \pm 1.1/2.5$ Ma, respectively (Fig. 13) and the isochron ages are concordant with the plateau ages (Fig. 13, Table 2). Sample ST-05-48 from the Padunskii sill is an analog of the previously dated sample 9/144y. It yielded an age of $241.6 \pm 1.3/2.6$ Ma (Ivanov et al., 2009), and overlaps within internal error with ST-05-48 (internal errors should be applied because different standards were used). Sample T2 yielded a plateau age of $240.1 \pm 1.0/2.5$ Ma, which is in agreement with the age of sample ST-05-4, if internal errors are applied. Thus, ages around 240 Ma are reproduced by dating of samples both treated by HF and HNO_3 and

analyzed after different irradiations, though measured in the same laboratory.

Fig. 14 shows $^{40}\text{Ar}/^{39}\text{Ar}$ results for sample ST-04-34 yielded a plateau age of $255.8 \pm 4.7/5.3$ Ma and concordant isochron age of $260.4 \pm 12.7/12.9$ Ma, although the errors are large; the initial $^{40}\text{Ar}/^{36}\text{Ar}$ has an atmospheric composition (Fig. 14, Table 2). Despite the large analytical error for this sample, the age is Late Permian and is statistically different from the Middle Triassic ages for the samples ST-05-4 and ST-05-48. Interestingly, the plateau age is similar to the Permian or Permo-Triassic age (254.2 ± 2.3 Ma) obtained by U–Pb SHRIMP on zircons separated from sample ST-08-110 collected about 170 km to the south of ST-04-34 (Paton et al., 2010).

Thus, our new $^{40}\text{Ar}/^{39}\text{Ar}$ ages reveal the existence of dolerite sills of both Late Permian and Early–Middle Triassic age in the Angara-Taseevskaya syncline.

6. Geologic evidence for long duration of the STLIP: Tunguska syncline example

The absence of sediment and paleosols between lava flows in the Noril'sk region indicates volcanic events of extremely short duration. Available geochronologic (Renne and Basu, 1991; Venkatesan et al., 1997; Kamo et al., 2003; Reichow et al., 2009) and paleomagnetic data (Pavlov et al., 2011) for the same region are in good agreement with such an observation. However, it is not the case for some other regions of the Siberian Traps province. For example, the Tunguska syncline (Fig. 1) contains layers and lenses of sedimentary rock intercalated with volcanic and volcanoclastics in a number of places in the section. Evidence from the drill-hole 22P (see location in Figs. 1 and 2) indicate that the volcanism in this region started in Permian, where according to the Soviet Geological Survey (informative notes for the

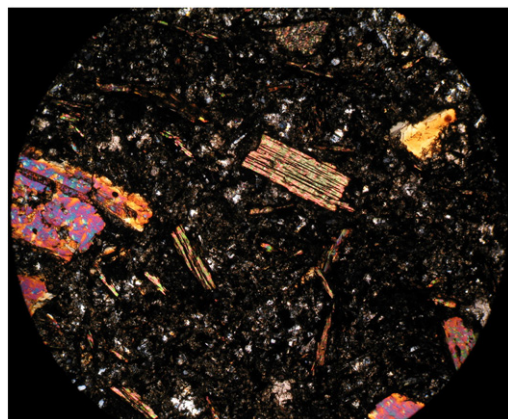


Fig. 8. Microphotograph of lamproite (sample ZP10). Cross-polarized light. Large crystals of phlogopite (up to few mm in length) are in leucite-rich matrix. Size of the view field is 4.4 mm across.

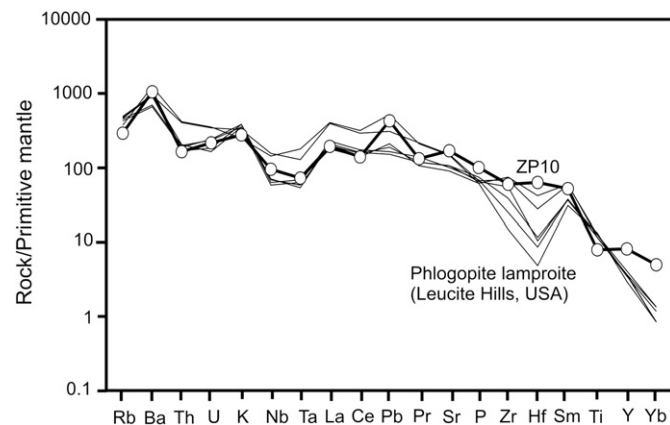


Fig. 9. Trace element patterns of a lamproite sample ZP10 compared to phlogopite lamproites from the Leucite Hills (Mirnejad and Bell, 2006). Trace element abundances are normalized to the primitive mantle composition of McDonough and Sun (1995).

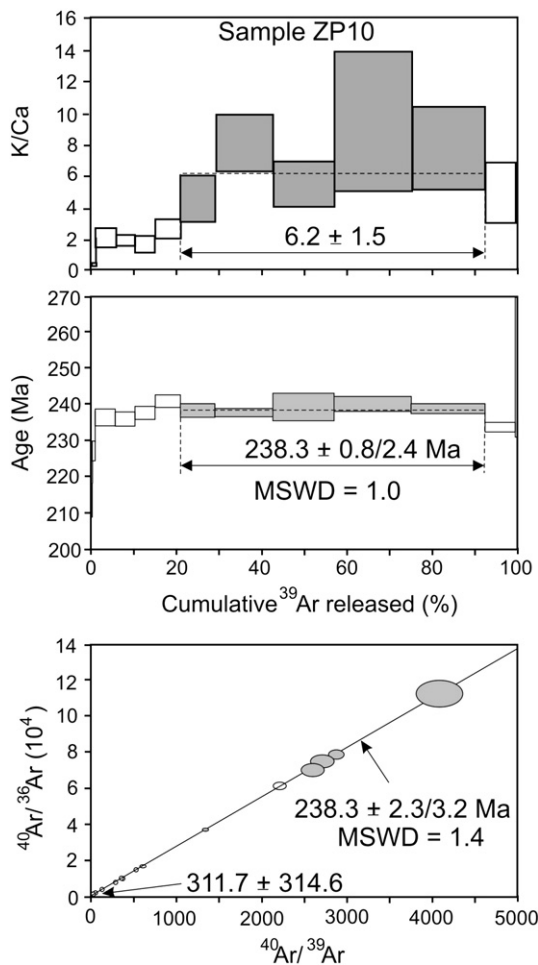


Fig. 10. Stepwise heating argon release spectrum and isochron diagram for a phlogopite separate of a lamproite sample ZP10 analyzed at the Institute of Geology and Geophysics CAS (Beijing, China). Error bars in the diagrams are analytical at the 2-sigma level. Steps used for calculations of the plateau age are shown in gray. The sample was treated by HF.

geologic map P-47-III by the USSR nomenclature) drill-hole 22P penetrated Permian coal-bearing sediments and tuffs. A 32 m thick tuff horizon embedded into the upper part of the Permian sediments forms an anticline structure and crop out at few localities along the Lower Tunguska. Few tens of meters of tuffs and tuffite horizons of the Tutonchansky and Korvuchansky suites, presumably of Triassic or Late Permian age, lie above. The tuffs and tuffites are covered by younger volcanic and sedimentary units of the Nidymsky, Kochechumsky and Jambukansky suites. Thickness of the tuffs and tuffites is variable and in some localities it exceeds half of a kilometer (Fig. 15). It is not evident where the Permo-Triassic boundary should be located. Traditionally, however, it is placed either within the volcanoclastic Korvuchansky suite or within the lava-dominated Nidymsky suite. $^{40}\text{Ar}/^{39}\text{Ar}$ ages of 248.9 ± 1.2 Ma and 251.8 ± 1.5 Ma were obtained for two different samples of the Lower Nidymsky sub-suite (exact location is not provided by Reichow et al., 2009). Within uncertainty these two ages bracket the $^{40}\text{Ar}/^{39}\text{Ar}$ age for the Permo-Triassic boundary or are slightly older than that boundary, respectively (Reichow et al., 2009). So, the Permo-Triassic boundary is most likely somewhere within the lower sub-suite of the Nidymsky suite.

From the cross-section shown in Fig. 15, it is evident that after the Permo-Triassic boundary there were two significant hiatuses in volcanism, during which sediments (mainly sandstones and argillites) were

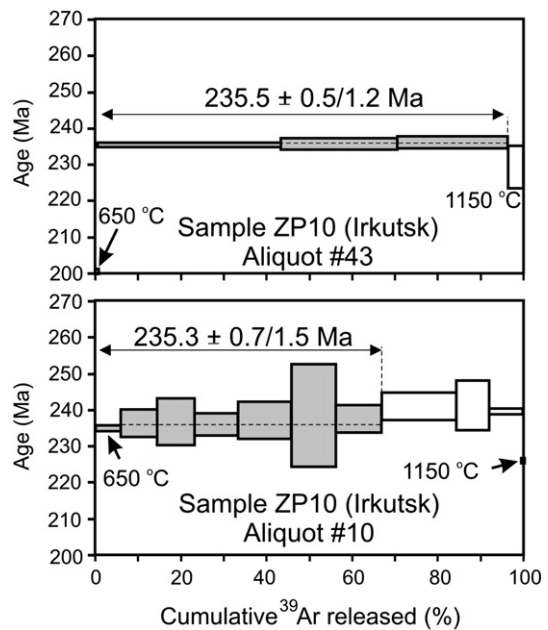


Fig. 11. Stepwise heating argon release spectra for phlogopite separates of a lamproite sample ZP10 analyzed at the Institute of the Earth's Crust SB RAS (Irkutsk, Russia). Aliquot number refers to the sample position in ampoule at the irradiation. Error bars in the diagrams are analytical at the 2-sigma level. Steps used for calculations of the plateau age are shown in gray. Temperatures of the first and last steps are shown for reference.

formed. The Upper Nidymsky suite and the Kochechumsky suite have not yet been dated. However, if we assume that Honna-Makitsky suite at Lake Khantaiskoe, located just above a stratigraphic discontinuity (Fig. 4) is an analog for the Upper Nidymsky suite, then we can infer an $^{40}\text{Ar}/^{39}\text{Ar}$ age of $240.9 \pm 1.3/2.6$ Ma (sample XA-39, Table 2) for it.

7. Review of geochronologic and paleomagnetic data for the STLIP

7.1. $^{40}\text{Ar}/^{39}\text{Ar}$ ages

In Table 3 we list selected $^{40}\text{Ar}/^{39}\text{Ar}$ ages published for the Siberian Traps. We have chosen ages from Baksi and Farrar (1991), Renne and Basu (1991), Dalrymple et al. (1995), Renne (1995), Basu et al. (1995), Venkatesan et al. (1997), Reichow et al. (2002, 2009), Ivanov et al. (2005, 2009) and this study. Ages from our own studies (Ivanov et al., 2005, 2009, this study) were scrutinized and only those ages that passed the chi-square test were selected. For ages from other studies we followed the interpretation of the original papers and selected those ages that were considered as "good" or "preferred". For example, Dalrymple et al. (1995) classified their ages on the basis of descriptive characteristics ("good", "fair", "poor" and "none") of the plateau in the argon-release spectra. From this study we have taken all ages with "good" plateaus, except for those ages obtained on biotites from the Noril'sk-1 intrusion, because the latter were shown to be affected by excess argon (Renne, 1995). Thus, ages obtained in a complementary study (Renne, 1995) for the Noril'sk-1 intrusion, which accounted for the excess argon, were used instead of ages of Dalrymple et al. (1995) (Table 3). The ages from Baksi and Farrar (1991) were left in Table 3 despite the fact that they were considered too young by Baksi (2007a,b) because of radiogenic argon loss. These ages will be considered separately, together with ages from Walderhaug et al. (2005), which were not included in Table 3 because of their disturbed argon-release spectra. Some other published ages (e.g. Vrublevskii et al., 2004; Fedoseev et al., 2005) were not included in Table 3, nor discussed, because they were obtained relative to the standard MCA-11, which is not calibrated against standard GA1550.

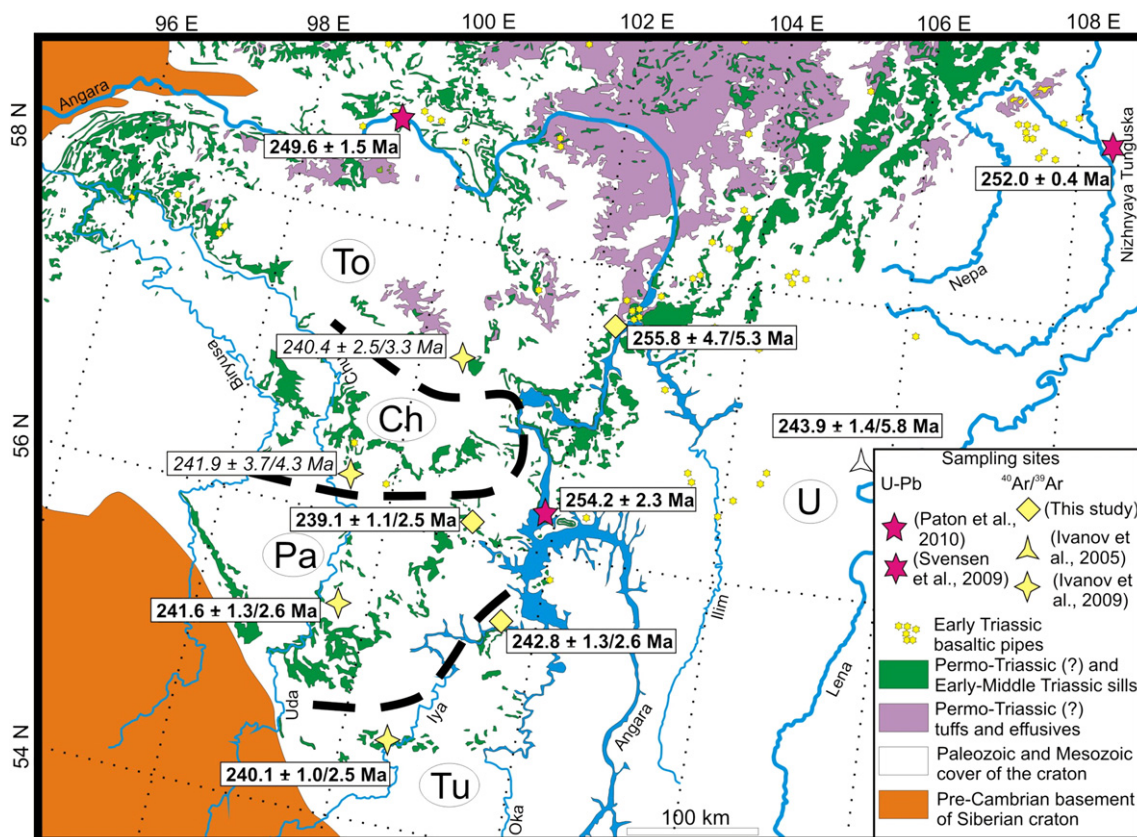


Fig. 12. Geologic map of the Angara-Taseevskaya syncline and adjacent areas (simplified after Malitch (1999)). Bold dashed lines outline the distribution of dolerite sills according to Feoktistov (1978). Abbreviations: Ch – Chuna-Biryusinskii sill; To – Tolstomysovskii sill; Pa – Padunskii sill; Tu – Tulunskii sill; U – Usol'skii sill. Also shown are the locations of samples dated by $^{40}\text{Ar}/^{39}\text{Ar}$ (Ivanov et al., 2005, 2009) and U–Pb (Svensen et al., 2009; Paton et al., 2010). Ages in italic are integrated step $^{40}\text{Ar}/^{39}\text{Ar}$ ages, which do not pass the chi-square test.

All ages listed in Table 3 are recalculated according to the method described by Spell and McDougall (2003) to be consistent with the 98.79 Ma age for standard GA1550 (Renne et al., 1998). Errors are not multiplied, however, because all necessary information was not always given in the original publications. Thus, minor mismatches (generally less than 1%) may exist between the final ages used from different studies. For example, when dating samples ST-04-4, ST-04-34 and ST-04-48 we used standard TCs with an age of 28.34 (± 0.085) Ma. Reichow et al. (2009) reported for the same standard an age of 28.24 (± 0.02) Ma. Therefore, the listed errors in Table 3 are underestimates. This underestimation of errors leads to the appearance of small peaks in Fig. 16. Major peaks, however, remain centered at ~250 Ma, ~241 Ma, ~232 Ma, and ~224 Ma with a probable peak at ~253 Ma, and these are not changed by the error underestimation.

The Late Permian peak at ~253 Ma is defined by ages obtained on micas for the West Siberian Basin (Reichow et al., 2002) and the Arydzhansky suite of the Maimecha-Kotuy province (Basu et al., 1995). Mica-based $^{40}\text{Ar}/^{39}\text{Ar}$ ages are under suspicion, however. It was shown by Renne (1995) that the Late Permian mica-based $^{40}\text{Ar}/^{39}\text{Ar}$ age of the Noril'sk-1 intrusion was an artifact due to the presence of excess argon in mica. However, the peak at ~253 Ma overlaps our new $^{40}\text{Ar}/^{39}\text{Ar}$ age of 255.8 \pm 4.7 Ma obtained on the matrix of sample ST-04-34 from the Angara-Taseevskaya syncline (Fig. 14).

The Permo-Triassic peak at ~250 Ma represents the major pulse of the Siberian flood basalt volcanism. Since many studies focused on this pulse of volcanism, it is not discussed here (e.g. Renne and Basu, 1991; Basu et al., 1995; Venkatesan et al., 1997; Reichow et al., 2002, 2009).

Middle Triassic volcanism at about 241 (± 3) Ma appeared in the Angara-Taseevskaya syncline (Ivanov et al., 2005, 2009; this study), at Chelyabinsk near the Urals (Reichow et al., 2009) and in the Central Putorana region (this study) (Fig. 1). Ages of 245.8 \pm 1.2 Ma and 238.6 \pm 0.8 Ma have been reported by Dalrymple et al. (1995) for the Avamsky dyke in the Kamensk region (see location in Fig. 2) and for the Dal'dykan sill in the Noril'sk-Kharaelakh region, respectively (Table 3). The majority of rocks of this age have trace element abundances that are similar to the flood basalts erupted during the major Permo-Triassic pulse (see Ivanov et al., 2009 and Figs. 5 and 6 in this paper). The volume of lava in the Central Putorana region (1.8–3.75 $\times 10^5$ km³), which belongs to this pulse of volcanism, exceeds the minimal volume for a large igneous province (see Section 4.2). The intrusion volumes in the Angara-Taseevskaya syncline are about 0.7 $\times 10^5$ km³ (Vasil'ev et al., 2000). The volume of lava at Chelyabinsk cannot be estimated at present. However, the Middle Triassic pulse of volcanism should be considered as a second pulse of flood basalt volcanism of the Siberian Traps province.

The Middle Triassic peak at ~232 Ma is based on a single age obtained by Baksi and Farrar (1991) for basalts in the Tunguska region (Figs. 2 and 3). As mentioned above, Baksi (2007a,b) considered this age erroneous on the basis of his alteration index criterion. It should be mentioned however, that a paleomagnetic study of Walderhaug et al. (2005) in the Taimyr region supports the existence of Middle Triassic basaltic magmatism.

The Late Triassic peak at ~224 Ma is due to the age of the Bolgokhtokh granite intrusion in the Noril'sk-Kharaelakh region (Dalrymple et al., 1995). No basalts with such ages are known in the Siberian Traps province.

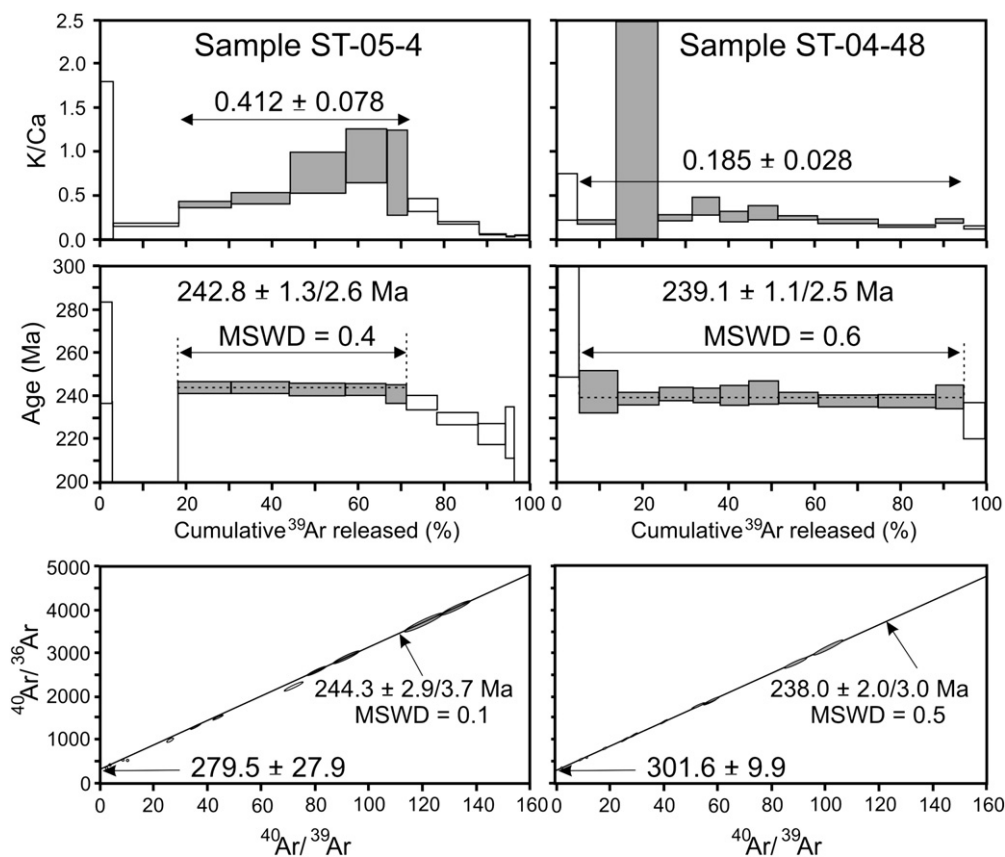


Fig. 13. Stepwise heating argon release spectra and isochrons for plagioclase separates of basaltic samples ST-05-4 and ST-05-48. Error bars in diagrams are analytical at the 2-sigma level. Steps used for calculations of plateau and isochron ages are shown in gray. Both samples pass the chi-square test for statistical significance of the plateau and isochron ages.

In summary, it is obvious that Siberian flood basalts were not erupted simultaneously at the Permo-Triassic boundary. There was probably an earlier, Late Permian pulse of volcanism, and followed thereafter by a later Middle Triassic pulse or a number of Triassic pulses. The latest event corresponds to the Late Triassic granitic magmatism.

7.2. U–Pb ages

U–Pb ages obtained for basalts, mafic and carbonatitic intrusions and granitic rocks are summarized in Table 4 and plotted in Fig. 17. Three age peaks can be seen: a Permo-Triassic peak at about 251 Ma, Middle Triassic peak at about 241 Ma and Late Triassic peak at about 229 Ma (Fig. 17). The same three peaks are also evident from the $^{40}\text{Ar}/^{39}\text{Ar}$ ages (Fig. 16), keeping in mind a systematic difference of about 1% between the U–Pb and $^{40}\text{Ar}/^{39}\text{Ar}$ timescales (Min et al., 2000). Some mismatches between the U–Pb and $^{40}\text{Ar}/^{39}\text{Ar}$ ages do exist. For example, the center of the Permo-Triassic peak of the Siberian flood basalt volcanism perfectly coincides with the Permo-Triassic stratigraphic boundary in the $^{40}\text{Ar}/^{39}\text{Ar}$ timescale (Fig. 16), but it follows the Permo-Triassic stratigraphic boundary in the U–Pb timescale (Fig. 17). The U–Pb age for the Bolgokhtokh intrusion is older than the $^{40}\text{Ar}/^{39}\text{Ar}$ age for the same intrusion, in excess of 1% of the systematic difference (Tables 3 and 4). However, such differences do not change the major point of this paper, namely that the Siberian Traps were formed by more than one Permo-Triassic pulse of magmatism. Importantly, the Permo-Triassic and Middle Triassic pulses of felsic magmatism were coeval with the two pulses of flood basalt volcanism. Late Triassic granitic magmatism did not have its basaltic counterpart. The Late Permian and Middle Triassic pulses of magmatism are borne out by the $^{40}\text{Ar}/^{39}\text{Ar}$ ages, but are not evident from the U–Pb data.

7.3. Paleomagnetic data

Paleomagnetic study in the Noril'sk-Kharaelakh region has shown that basaltic volcanism started in the latest Late Permian during a reverse chron and continued during normal chron at the beginning of the Early Triassic (e.g. Heunemann et al., 2004). This is in agreement with the very short (<1 Ma) duration of volcanism in this region as deduced from the $^{40}\text{Ar}/^{39}\text{Ar}$ ages (see Fig. 3). However, paleomagnetic data from other regions suggest that the overall duration of Siberian Traps magmatism was longer. The most important paleomagnetic evidence for a long duration of magmatism was obtained from the study of the super deep drill-hole SG6 (see location in Fig. 1). There, five normal and four reverse chrons were revealed (Kazanskii et al., 2000), which suggest a duration of about 9 Ma (Steiner, 2006). As mentioned in Section 7.1, paleomagnetic data for some Taimyr dolerite sills suggests their emplacement in the Middle Triassic (Walderhaug et al., 2005), implying an overall duration of up to 10–30 Ma. Reviewing paleomagnetic data obtained for the Siberian Traps, Steiner (2006) concluded that “revised magnetostratigraphic correlation of the Siberian igneous rocks has enormous significance, in that it indicates that the Siberian flood basalt volcanism did not occur simply at the time of the mass extinction, but was ongoing in the Late Permian, that it spanned the Permian–Triassic boundary, and that it continued into the Early Triassic” (Steiner, 2006, p. 33).

8. Duration of the Siberian Traps magmatism in comparison with other large igneous provinces

The most comprehensive review up to now on timing of the large igneous provinces magmatism was provided by Bryan and Ernst (2008). See that paper for a more complete list of references.

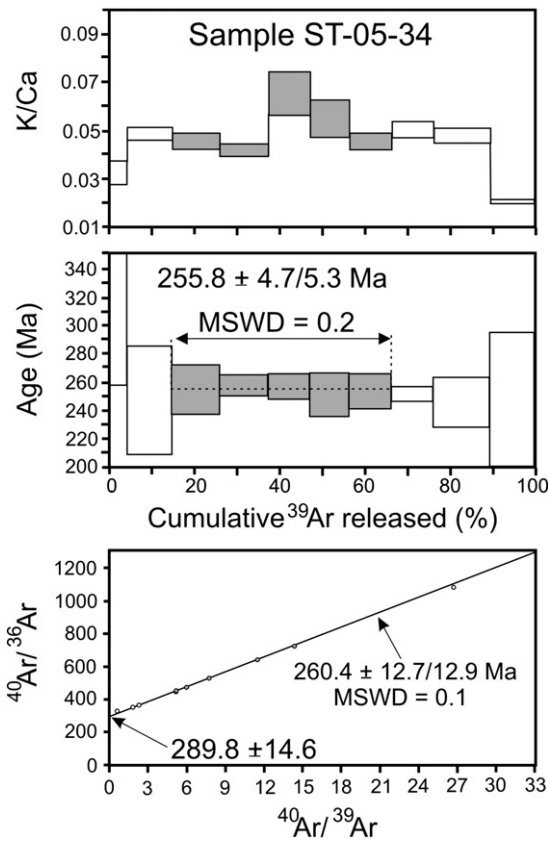


Fig. 14. Stepwise heating argon release spectra and isochrones for the matrix separate of basaltic sample ST-05-34. Error bars in diagrams are analytical at the 2-sigma level. Steps used for calculations of plateau and isochron ages are shown in gray. The ages pass the chi-square test for statistical significance of the plateau and isochron ages.

In their revision, Bryan and Ernst (2008) have shown that significant varieties exist among large igneous provinces. First, some of them are composed of mafic rocks, vary in duration from very short (few Ma) to long (up to 40–60 Ma) with majority of the provinces having durations averaging about 15 Ma. Third, in general magmatism of felsic large igneous provinces (silicic according to original definition of Bryan and Ernst, 2008) lasts longer than mafic large igneous provinces. And finally,

short-lived large igneous provinces are typically single-pulsed, whereas long-lived large igneous provinces were formed by number of pulses.

The Siberian Traps province falls between mafic and felsic end-members. It contains both mafic and felsic rock, though basalts are major rock-types. It is longer lived than pure mafic large igneous provinces, but it is not as long as the longest felsic large igneous provinces. As a typical long-lived large igneous province, it had at least two pulses of mafic volcanism, and at least three pulses of the felsic magmatism.

We note, however, that such comparisons should be done with some caution because the compilation of Bryan and Ernst (2008) may contain some incomplete and/or incorrect data entries. For example, they considered the Siberian Traps province as short (<2 Ma) and single pulsed, whereas we argue that it was long and multi-pulsed. An opposite case could also exist. The Karoo flood basalt province was considered as multi-pulsed with more than 6 Ma of history based on $^{40}\text{Ar}/^{39}\text{Ar}$ dating (Jourdan et al., 2008), but later U–Pb dating revealed only a single pulse of short duration (Svensen et al., 2012). Similarly, duration of Emeishan flood basalt volcanism was shortened to less than 2 Ma using high precision chemical abrasion TIMS U–Pb data (Shellnutt et al., 2012).

Thus, the geologic constraints, such as interlayering of lava and sediments (or absence of such interlayering) and paleomagnetic studies are of particular importance in distinguishing between short and long-lived large igneous provinces. Using such constraints, it was shown that Deccan Traps were formed in the latest Cretaceous and earliest Paleogene during two major pulses separated by 1–2 Ma (Courtilot et al., 2000; Chenet et al., 2008), but minor basaltic volcanism occurred several Ma earlier (Chenet et al., 2008) and felsic volcanism continued later extending the total duration of the Deccan Traps from 67.5 Ma to 60 Ma (Sheth et al., 2001).

Geologic, paleomagnetic and geochronologic data for the Siberian Traps province suggest that in terms of duration it is rather more similar to Deccan Traps than to Karoo and Emeishan provinces.

9. Discussion

9.1. Geodynamic implications

Various models have been discussed for the origin of the Siberian flood basalt province: starting plume head (Campbell and Griffiths, 1990), thermochemical plume (Lin and Van Keken, 2005; Dobretsov et al., 2008; Sobolev et al., 2011), lithosphere delamination (Elkins-Tanton, 2005), convection reorganization at a craton edge (King and Anderson,

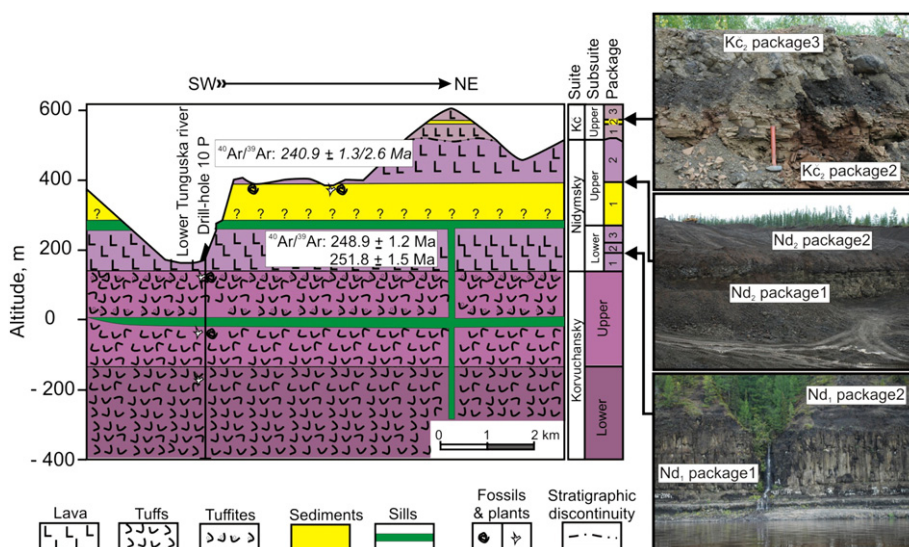


Fig. 15. Geologic cross-section at the Tura settlement (see Fig. 2 for location). Suite names are taken from geologic map Q-47-XXXV (according to the USSR nomenclature), and subdivisions to packages are from authors' field observations. The Nd₁ package 2 is composed of the pillow lavas. The Nd₁ package 2 and Kochechumsky (Kč) package 3 contain pillow lava horizons just on the top of the sedimentary horizons. The $^{40}\text{Ar}/^{39}\text{Ar}$ age for the upper Nidymysky suite is by correlation.

Table 3
Selected $^{40}\text{Ar}/^{39}\text{Ar}$ ages for Siberian Traps. All ages are recalculated in accordance with the procedure of Spell and McDougall (2003) to be consistent with the age of 98.79 Ma for the GA1550 standard (Renne et al., 1998).

Reference for original study	Used standard and its age (Ma) in original study	Sample number	Age of the sample (Ma)	Age of the standard to be consistent with age of 98.79 Ma for GA1550 (Ma)	Recalculated age of the sample
Baksi and Farrar (1991)	SB3, 162.9	ES154	238.4 ± 1.4	164.6 ^a	241.0 ± 1.4
		ES524	229.9 ± 2.3		232.4 ± 2.3
Renne and Basu (1991)	FCs, 27.84	46	248.4 ± 0.3 ^b	28.02	250.0 ± 0.3
		42	247.5 ± 1.1 ^b		249.1 ± 1.1
		2	247.5 ± 0.7		249.1 ± 0.7
Dalrymple et al. (1995)	TCs, 27.92	SG-32-2328	244.1 ± 1.2	28.34	247.8 ± 1.2
		SG-32-2515.4	244.4 ± 1.2		248.1 ± 1.2
		NP-25-596.4	245.4 ± 1.2		249.1 ± 1.2
		90ZUBC4	235.0 ± 0.8 ^b		238.6 ± 0.8
		AV2	244.7 ± 1.2		245.8 ± 1.2
		BG-26	223.2 ± 0.8 ^b		224.2 ± 0.8 ^b
Renne (1995)	FCs, 28.03	7231bio	250.0 ± 1.2	28.02	249.9 ± 1.2
		7230amph	249.3 ± 1.6		249.2 ± 1.6
					249.6 ± 1.0 ^b
Basu et al. (1995)	FCs, 28.03	1946/23	253.3 ± 2.6	28.02	253.2 ± 2.6
		No number	249.88 ± 0.25 ^b		249.8 ± 0.3
Venkatesan et al. (1997)	MMhb-1, 520.4	SG9-1216	246.7 ± 1.9	523.1	248.2 ± 1.9
		MK-6	247.6 ± 2.5		249.1 ± 2.5
		86-64	247.1 ± 1.9		248.6 ± 1.9
		MK-15	249.1 ± 5.5		250.6 ± 5.5
		86-95	248.3 ± 1.7		249.8 ± 1.7
Reichow et al. (2002)	GA1550, 98.79	3c97-97	249.1 ± 0.8	98.79	249.1 ± 0.8
		3c97-45	249.7 ± 0.8		249.7 ± 0.8
Reichow et al. (2002)	GA1550, 98.79	3c97-8	249.3 ± 0.8	98.79	249.3 ± 0.8
		3c97-82	252.5 ± 1.5		252.5 ± 1.5
		3c97-81	253.4 ± 0.8		253.4 ± 0.8
Ivanov et al. (2005)	LP6, 129.4	2840 and 2848	243.9 ± 1.0 ^b	129.4	243.9 ± 1.0 ^b
Reichow et al. (2009)	FCs, 28.02	SG32-54.0	250.3 ± 1.0 ^b	28.02	250.3 ± 1.0 ^b
		SG32-2328.0	247.5 ± 0.8		247.5 ± 0.8
		SG32-2515.4	248.7 ± 0.6		248.7 ± 0.6
		91-58	251.8 ± 1.5		251.8 ± 1.5
		91-75	248.9 ± 1.2		248.9 ± 1.2
		S4.1	250.3 ± 0.7		250.3 ± 0.7
		FGS8	250.7 ± 0.6		250.7 ± 0.6
		FGS1	250.6 ± 0.4 ^b		250.6 ± 0.4 ^b
		FGS5	251.5 ± 0.4 ^b		251.5 ± 0.4 ^b
		T98-57	250.6 ± 0.9 ^b		250.6 ± 0.9 ^b
		T98-58	251.0 ± 0.7		251.0 ± 0.7
		322/4	247.4 ± 0.6		247.4 ± 0.6
		322/1	249.7 ± 0.7		249.7 ± 0.7
		7/254.0	243.3 ± 0.6		243.3 ± 0.6
		7/696.4	242.2 ± 0.4 ^b		242.2 ± 0.4 ^b
Ivanov et al. (2009)	Bern4M, 18.7	T2	240.1 ± 1.0	18.7	240.1 ± 1.0
		9/144y	241.6 ± 1.3		241.6 ± 1.3
This study	Bern4M, 18.7	XA39	240.9 ± 1.3	18.7	240.9 ± 1.3
	TCR, 28.34	ST-05-4	242.8 ± 1.3	28.34	242.8 ± 1.3
		ST-05-48	239.1 ± 1.1		239.1 ± 1.1
		ST-05-34	255.8 ± 4.7		255.8 ± 4.7
		ZP10	238.3 ± 1.3		238.3 ± 1.3

All errors are analytical and thus are underestimates.

^a Cross-calibration between two studies (Baksi et al., 1996; Renne et al., 1998) was used.

^b Average for two or more aliquots of the same sample or different samples taken from the same intrusion and collected in the same drill-hole.

1998), thermal blanketing by cratonic lithosphere (Coltice et al., 2007), and wet diapirs originating above a stagnant slab (Ivanov et al., 2008). This paper is devoted to the assessment of quality of geochronologic data, rather than assessment of the reliability of the models listed above. However, geochronologic information may give important constraints on some of the suggested models.

The starting plume head model predicts “a burst of basaltic volcanism sometime after maximum uplift is reached, with most of the magmas erupted early but continuing at a decreasing rate, perhaps for a period of the order of 20 Ma” (Campbell and Griffiths, 1990, p. 89). Indeed, the duration of the basaltic volcanism is at least 10 Ma and may be even 20 Ma as seen from the $^{40}\text{Ar}/^{39}\text{Ar}$ data (Fig. 16). However, no uplift was documented for the Siberian Traps region (Czamanske et al., 1998), and no volcanism was taking place continuously (or semicontinuously) while decreasing in rate, but occurred in a number of separate pulses. Thick

tuff units within the Tunguska syncline and pillow lavas of the package 2 of the Lower Nidymysky suite, as well as shallow water sedimentary deposits of the Upper Nidymysky and Kochechumsky suites with the pillow lava on top of them (Fig. 15) testify that the region was under sea level most of the time of volcanism.

Uplift was identified as one of the important predictions of the plume model (Campbell, 2005), and this leads to the debate on whether or not natural examples fit that prediction (e.g. Czamanske et al., 1998; Peate and Bryan, 2008; Ali et al., 2010; Sun et al., 2010). The uplift history as a response to plume arrival to the base of the lithosphere is controversial, however. Most modelers calculate that the region should be uplifted by about 0.6–2 km for the thermal plume (e.g. Campbell, 2005; Sobolev et al., 2011) (Fig. 18), and the uplift could be less pronounced if dense eclogite is entrained into such plume (Sobolev et al., 2011). Alternatively, Leng and Zhong (2010) modeled that the net effect

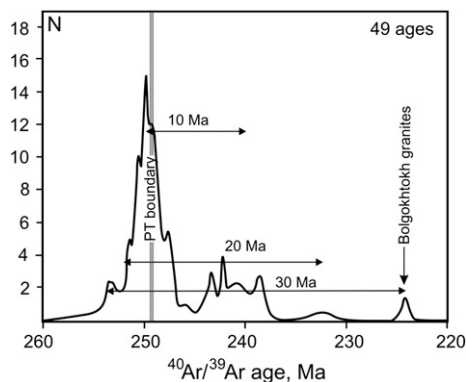


Fig. 16. Probability distribution of $^{40}\text{Ar}/^{39}\text{Ar}$ ages of the Siberian Traps. All ages are for basalts and their intrusive analogs, except the Bolgokhtokh granite intrusion and Noril'sk lamproite. Individual ages and data sources are listed in Table 3. The P–T boundary is after Reichow et al. (2009).

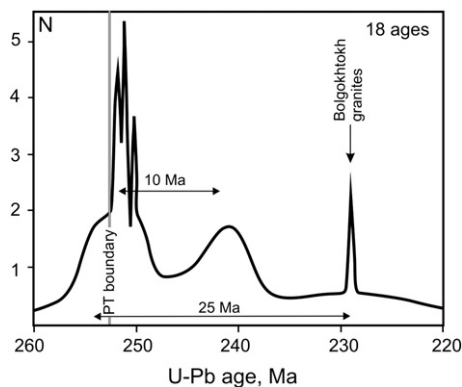


Fig. 17. Probability distribution of U–Pb ages of the Siberian Traps. Most of the ages are for granitic intrusions, except those with high precision near the Permo-Triassic boundary. Individual ages and data sources are listed in Table 4. The P–T boundary is after Mundil et al. (2004).

of plume arrival and basalt loading is subsidence, not uplift (Fig. 18). In addition to the controversies in modeling, natural factors, such as horizontal tectonic movements may create significant topographic anomalies larger than that due to plume arrival (Braun, 2010). Spatial distribution of the Siberian flood basalt province is such that any modeling curve could be fitted to pre-volcanic topography somewhere within the province, either to pre-volcanic subsidence at the Tunguska syncline or to pre-volcanic uplift at the Western Siberian Basin. After the Siberian flood basalt volcanism these two regions experienced opposite vertical movement; uplift of the Tunguska syncline and subsidence of the Western Siberian Basin.

Thermochemical plume modeling is also controversial. For example, Lin and Van Keken (2005) suggested a thermochemical plume model, according to which a thermal plume carries blocks of dense eclogite into the melting zone. Such model predicts episodic volcanism due to repeated ascent and sinking of dense eclogite within a rising mantle column. Such prediction would agree with the observed volcanic pulses. However, Sobolev et al. (2011) provided a model in which interaction of thermochemical plume and the lithosphere is very rapid. According to that model the thermochemical plume reached a depth of ~130 km within a thinned part of the cratonic lithosphere where eclogite began to melt. At that point andesitic to dacitic melt was produced to interact with the ambient peridotitic mantle and converted it to pyroxenite. Melting of the pyroxenite produced basaltic melts, which finally erupted on the surface (Sobolev et al., 2007). Some melts crystallized

within the lithosphere in the form of dense eclogite promoting Raleigh–Taylor instabilities and delamination (Elkins-Tanton, 2005). Due to delamination the plume material propagated to shallower levels where the peridotite began to melt (Fig. 19 left) (Sobolev et al., 2009). All these steps were modeled to occur within less than 1 Ma and according to the model the delamination stage took place after formation of the Gudchikhinsky suite but before the formation of the Tukulonsky suite (Sobolev et al., 2011). However, our $^{40}\text{Ar}/^{39}\text{Ar}$ results suggest that the lamproite dyke (sample ZP10) emplaced significantly later (by more than 10 Ma) than the formation of the Noril'sk lava sequence. Lamproites are deep melts produced generally from depths >130 km (>4 GPa) from veined lithospheric mantle keel (e.g. Mitchell, 1995). This suggests that the lithosphere of the Siberian craton remained thick and unperturbed, contrary to what is modeled by Sobolev et al. (2011). Thick lithospheric mantle beneath the Siberian craton without any signs of thinning is also evident from seismic data which suggest a lithospheric thickness of about 200 km everywhere within the Siberian craton (Priestley and McKenzie, 2006; Pasyanos, 2010). Thus, to melt the mantle below the cratons at a depth of about 200 km or deeper, one must assume significant fluxing of the mantle with water (Fig. 19 right) or other volatiles.

A somewhat different view of thermochemical plumes was provided by Dobretsov et al. (2008), who proposed that plumes are driven by buoyancy of a melt originated at the core mantle boundary. In their view a thermochemical plume is a relatively thin, tail-like

Table 4
Published U–Pb ages for basic intrusions and lava and granitic intrusions of the Siberian Traps.

Region	Intrusion/suite, rock type	Age (Ma)	Technique	Reference
Noril'sk-Kharaelakh Maimecha-Kotuy	Noril'sk-1, gabbro	251.2 ± 0.3	ID-TIMS	Kamo et al. (1996)
	Arydzhansky suite, basalt	251.7 ± 0.4 ^a	ID-TIMS	Kamo et al. (2003)
	Delkansky suite, basalt	251.1 ± 0.3		
	Guli carbonatites, basalt	250.2 ± 0.3		
Laptev sea Southeastern Tunguska syncline Angara-Taseevskaya syncline	Sills at Belkov isl., dolerite	252 ± 2	SIMS	Kuzmichev and Pease (2007)
	Sills at Nepa, dolerite	252.0 ± 0.4	ID-TIMS	Svensen et al. (2009)
	Padunskii sill (Bratsk), dolerite	254.2 ± 2.3	SHRIMP	Paton et al. (2010)
	Sill at Boguchany (Kodinsk), dolerite	249.6 ± 1.5		
Kuznetsk basin	Kolba intrusion, granite	256 ± 8	SHRIMP	Vladimirov et al. (2001)
		253 ± 4		
		245 ± 7		
	Monastyrsky intrusion, granite	231 ± 11		
	225 ± 4			
Noril'sk-Kharaelakh Kara sea	Bolgokhtokh intrusion, granite	229.0 ± 0.4	ID-TIMS	Kamo et al. (2003)
	Rastorguev isl., syenite	249.0 ± 5.2	SIMS	Vernikovskiy et al. (2003)
	Morzhov isl., syenite	242.0 ± 3.6		
Taimyr Eniseysky Kryazh	Uboinaya river, syenite	241.0 ± 6.5	SIMS	Vernikovskiy et al. (2003)
	Porozhnyi massif, trachyte	240 ± 3	SHRIMP	Vernikovskaya et al. (2010)

^a Dated mineral was perovskite.

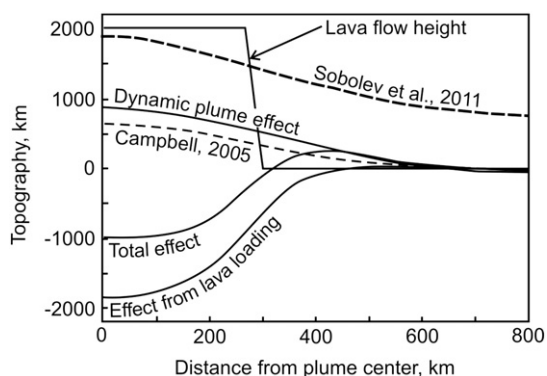


Fig. 18. Modeled topography for the case of dynamic plume effect and combination of the dynamic plume and basalt loading after Leng and Zhong (2010) (solid curves). For comparison topographic anomalies from dynamic plume effect are shown according to modeling of Campbell (2005) and Sobolev et al. (2011) (dashed curves). The figure shows that if the effect of basalt loading is accounted for, the total topography anomaly could be negative despite the fact that rising plume supports the positive topography.

structure, which attains its head upon collision with the lithosphere. This would predict radial spread of the plume material and time progression of the volcanism from the plume center. However, the available data on geochronology reviewed in this paper does not reveal such time progression.

This brief consideration of the plume models shows the existing difficulties of explaining the Siberian flood basalt volcanism. Another critical problem is enormous size of the province, about 4000 km across (Fig. 1), which is not explained by any of the models mentioned above. In addition one should be mindful that felsic magmas erupted both at the Permo-Triassic boundary and in the Middle Triassic during the two most voluminous pulses of basaltic volcanism, as well as in the Late Triassic following cessation of the basaltic volcanism. Thus an additional question should be considered: what is the relation between basaltic and felsic magmas? Was the felsic magmatism a consequence of the basaltic magmatism, or is it a separate phenomenon? If the former applies, then why are the acid magmas mainly situated in peripheral parts of the Siberian Traps province? If the latter applies, then

what mechanism caused two separate magmatic phenomena within the same period? To understand the origin of the Siberian Traps, future studies should focus on such problems.

9.2. Environmental impact

The Permo-Triassic environmental catastrophe was one of the most notable in Phanerozoic history, accounting for the extinction of 90% marine and 75% terrestrial species (Erwin, 1994). Generally speaking, external (extraterrestrial impact or volcanism) and intrinsic causes (sea level changes, anoxia or climatic changes) of the mass-extinctions are usually acknowledged (Hallam and Wignall, 1997; Racki, 2003; Keller, 2005). Below we consider only 'external' models, because the chronology of the Siberian Traps, which is the main topic of this paper, cannot be applied for testing the 'intrinsic' models.

The extraterrestrial impact model flourished from the seminal paper by Alvarez et al. (1980), which linked globally-distributed layer with Ir anomaly at the K-T boundary to high concentrations of this element in majority of the meteorites and later realization that the Ir anomaly has direct link to the Chicxulub buried crater (Hildebrand et al., 1991). Being the most popular, though not universally accepted model for the K-T mass extinction (see Schulte et al., 2010 vs Keller et al., 2010), the impact hypothesis is thought to be inconsistent with the P-T mass extinction (Courtillot and Renne, 2003). There were some attempts to find evidence of impact at the Permo-Triassic boundary with controversial results (e.g. Kaiho et al., 2001 vs Koeberl et al., 2002; Becker et al., 2004 vs Glikson, 2004). Recently a 40-km diameter Araguainha impact crater with an age about the same as the age of the Permo-Triassic boundary was found in Brasilia (Tohver et al., 2012). However, no anomalously high concentrations of Ir and other PGEs were found in the Permo-Triassic boundary oceanic sediments (Brookfield et al., 2010) (Fig. 20) suggesting that either the Araguainha projectile was an achondrite or icy comet (so it had no elevated PGE concentrations) or the age of the impact did not coincide with the Permo-Triassic boundary.

A volcanic model for the mass-extinctions is based on coincidence of the flood basalt eruptions with every five Phanerozoic great mass-extinctions (namely, end-Ordovician, Permo-Triassic, latest Triassic,

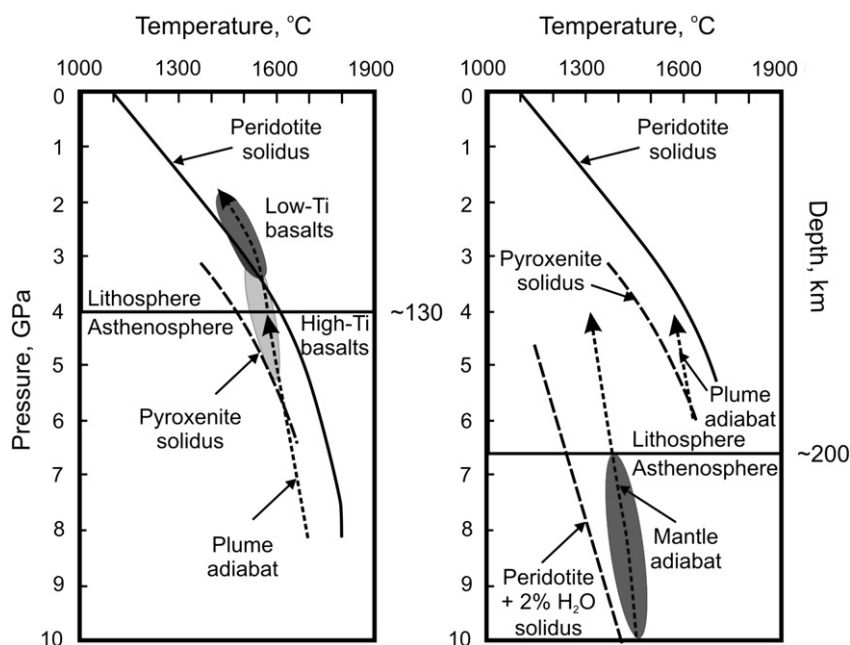


Fig. 19. PT diagram showing the essential steps of melting of a dry plume in the model of Sobolev et al. (2011). (The figure in the left is reproduced from Sobolev et al., 2009 with minor modifications). However, if the lithospheric mantle was significantly thicker than 130 km, as would be expected from seismic data of the modern lithospheric thickness of about 200 km for the Siberian craton (Priestley and McKenzie, 2006; Pasyanos, 2010), the sublithospheric mantle could be melted only if plume was fluxed with water or other volatiles. The wet solidus in the right figure is after Litasov and Ohtani (2003).

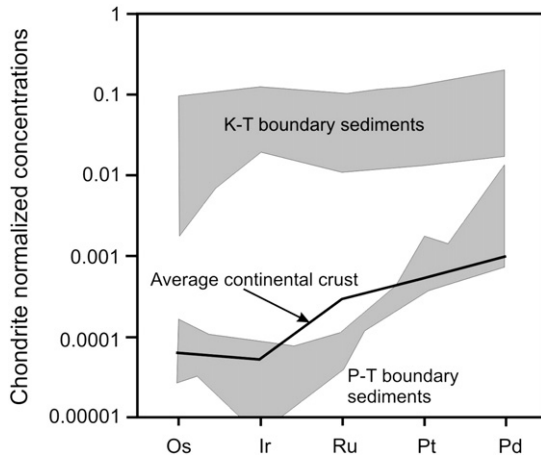


Fig. 20. Chondrite normalized concentration of platinum group elements in sediments at the K–T and P–T boundaries in comparison with average continental crust. Data are after Kyte et al. (1985), Peucker-Ehrenbrink and Jahn (2001), Lee et al. (2003), Brookfield et al. (2010), and Ivanov et al. (submitted for publication). Values for normalization are after McDonough and Sun (1995).

Cretaceous–Tertiary and Late Eocene) (Courtilot and Renne, 2003). However, the killing mechanism of the flood basalt eruptions is not well understood. Usually, the toxic gas loading to the atmosphere

from the volcanic eruptions (Self et al., 2005) and magma interaction with organic-rich sediments (Svensen et al., 2004) is considered. For example, Black et al. (2012) considered that atmospheric load from the Siberian Traps could be as large as 6300–7800 Gt of S, 3400–8700 Gt of Cl and 7100–13,600 Gt of F. In order to consider these loads to be a controlling factor for the mass-extinction, these elements converted to toxic gasses should be erupted into the atmosphere just before and/or at the time of the mass-extinction. Fig. 21 compares the timing of the mass-extinctions in the vicinity of the Permo-Triassic boundary with timing of the Emeishan and Siberian Traps flood basalt eruptions. If we base our consideration on U–Pb ages solely, which are, on one hand, analytically more precise and, on the other hand, usually considered as more reliable compared to the $^{40}\text{Ar}/^{39}\text{Ar}$ ages, we note that majority of the flood basalt eruptions took place after the mass-extinction events (see also Fig. 17). In this case, then, we cannot consider any supposed effect from the calculated gas loading which took place after the mass-extinction as the killing and/or triggering mechanism for the mass-extinctions. However, if we use $^{40}\text{Ar}/^{39}\text{Ar}$ ages for both the Permo-Triassic boundary and the Siberian flood basalt eruptions, then pulse 1 of the Siberian flood basalt volcanism corresponds directly to the timing of the Permo-Triassic boundary (Figs. 16 and 21).

Such inconsistency between U–Pb and $^{40}\text{Ar}/^{39}\text{Ar}$ ages is not an artifact of decay constants used because we do not compare U–Pb and $^{40}\text{Ar}/^{39}\text{Ar}$ ages directly, but instead we compare time differences on the U–Pb and $^{40}\text{Ar}/^{39}\text{Ar}$ time scales. Here we propose a new explanation for

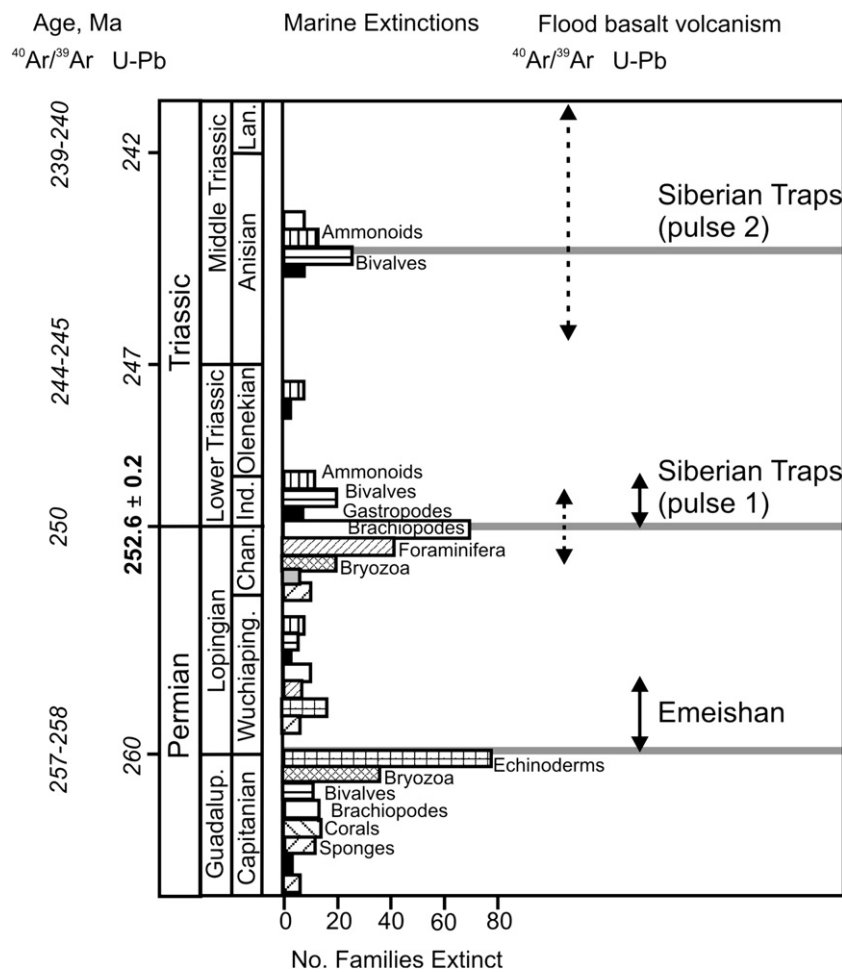


Fig. 21. Faunal turnover from the Permian to Middle Triassic compared to timing of the Emeishan and Siberian Traps flood basalt volcanism. Age values for the U–Pb time scale are rounded values after Mundil et al. (1996) and Gradstein et al. (2012) except the age for the Permo-Triassic boundary after Mundil et al. (2004). Age values for the $^{40}\text{Ar}/^{39}\text{Ar}$ time scale are rounded values using Reichow et al. (2009) age for the Permo-Triassic boundary and assuming ~2–3 Ma difference between the U–Pb and $^{40}\text{Ar}/^{39}\text{Ar}$ ages. Faunal data modified by Keller (2005) after Hallam and Wignall (1997). Spread of the columns with number of extinct families over the Y-axis is artificial. Timing of the extinctions is marked by horizontal gray strips. Timing of the Emeishan and Siberian Traps flood basalt volcanism is after Shellnutt et al. (2012) and this work, respectively. Solid and dashed vertical lines with arrows refer to U–Pb and $^{40}\text{Ar}/^{39}\text{Ar}$ time constraints on the volcanism, respectively.

this discrepancy between the U–Pb and $^{40}\text{Ar}/^{39}\text{Ar}$ ages not yet considered before by any other studies.

Dated zircons from ash layers in sedimentary sequences, such as Meishan stratotype section in east China, likely were not the ashes from the flood basalt eruptions, but rather were ashes from SiO_2 -rich arc volcanoes (flood basalts contain very little zircons, whereas acid arc magmas are zircon-rich). Arc volcanoes may have long-lived crustal magmatic chambers, where zircons crystallized few hundreds of thousands of years in advance of the eruption. Thus, zircons from sedimentary sections may be slightly too old compared to time of the sedimentation.

An additional and probably a more important source of toxic gases could be thermogenic gases that originated due to interaction of hot magma and organic- and chlorine-rich sediments during sill emplacements (Svensen et al., 2009). Our results on the $^{40}\text{Ar}/^{39}\text{Ar}$ dating of the sills in the Angara-Taseevskaya syncline show that some sills were emplaced during the second pulse of the Siberian flood basalt eruptions. If the mechanism proposed by Svensen et al. (2009) is correct, and if the $^{40}\text{Ar}/^{39}\text{Ar}$ ages are also correct, we might expect one more mass-extinction event in the Middle Triassic. Indeed more than 20% of the bivalves and over than 10% of the ammonoids became extinct in the Middle Triassic, supporting this idea (Fig. 21).

10. Conclusions

Siberian Traps constitute a large igneous province that was formed by eruptions of magma of both basaltic and felsic composition. Geological data provide clear evidence that volcanism initiated in the Permian and continued to the Triassic with at least one or two significantly long gaps between the volcanic pulses. Geochronologic data show that voluminous basaltic eruptions (flood basalts) took place at least twice: at the Permo-Triassic boundary (~249 Ma or 252 Ma using the $^{40}\text{Ar}/^{39}\text{Ar}$ and U–Pb timescales, respectively) and about 10 Ma later in the Middle Triassic. It is likely that less voluminous basaltic eruptions also occurred in latest Permian times, a few million years before the Permo-Triassic boundary, as well as in the Middle Triassic. However, the reliability of these ages should be assessed separately. Felsic magmatism accompanied basaltic magmatism of the two flood basalt episodes, and the latest episode of the felsic magmatism took place in the Late Triassic.

Acknowledgments

The paper benefited from constructive reviews by Ray Macdonald and anonymous reviewer and editorial comments. Wally Bothner helped with English and terminology usage. The work was sponsored by the Siberian Branch of the Russian Academy of Sciences (project no. 6) and partially by the Russian Ministry of Science and Education (grant 2012-1.5-12-000-1006-001). A.V.I. is thankful for the visiting scientist grant from Paleomagnetism and Geochronology Laboratory of the Institute of Geology and Geophysics (Chinese Academy of Sciences, Beijing). This is Argus VI (Irkutsk) publication number 1.

Appendix A. Supplementary data

Supplementary data to this article can be found online at <http://dx.doi.org/10.1016/j.earscirev.2013.04.001>.

References

Al'mukhamedov, A.I., Medvedev, A.Ya., Zolotukhin, V.V., 2004. Chemical evolution of the Permian–Triassic basalts of the Siberian platform in space and time. *Petrology* 12, 297–311.

Ali, J.R., Fitton, J.G., Herzberg, C., 2010. Emeishan large igneous province (SW China) and the mantle-plume up-doming hypothesis. *Journal of the Geological Society* 167, 953–959.

Alvarez, L.W., Alvarez, W., Asaro, F., Michel, H.V., 1980. Extraterrestrial cause for the Cretaceous-Tertiary extinction - experimental results and theoretical interpretation. *Science* 208, 1095–1108.

Baksi, A.K., 2007a. A quantitative tool for detecting alteration in undisturbed rocks and mineral - I: water, chemical weathering and atmospheric argon. In: Foulger, G.R., Jurdy, D.M. (Eds.), *Plates, Plumes and Planetary Processes: Geological Society of America Special Paper*, 430, pp. 285–304.

Baksi, A.K., 2007b. A quantitative tool for detecting alteration in undisturbed rocks and mineral - II: application to argon ages related to hotspots. In: Foulger, G.R., Jurdy, D.M. (Eds.), *Plates, Plumes and Planetary Processes: Geological Society of America Special Paper*, 430, pp. 305–333.

Baksi, A.K., Farrar, E., 1991. $^{40}\text{Ar}/^{39}\text{Ar}$ dating of the Siberian Traps, USSR: evaluation of the ages of the two major extinction events relative to episodes of flood-basalt volcanism in USSR and the Deccan Traps, India. *Geology* 19, 461–464.

Baksi, A.K., Archibald, D.A., Farrar, E., 1996. Intercalibration of $^{40}\text{Ar}/^{39}\text{Ar}$ dating standards. *Chemical Geology* 129, 307–324.

Basu, A.R., Poreda, R.J., Renne, P.R., Teichmann, F., Vasiliev, Yu. R., Sobolev, N.V., Turrin, B.D., 1995. High- ^3He plume origin and temporal-spatial evolution of the Siberian flood basalts. *Science* 269, 822–825.

Becker, L., Poreda, R.J., Basu, A.R., Pope, K.O., Harrison, T.M., Nicholson, C., Lasky, R., 2004. Bedout: a possible end-Permian impact crater offshore of northwestern Australia. *Science* 304, 1469–1476.

Black, B.A., Elkins-Tanton, L.T., Rowe, M.C., Ukstins Peate, I., 2012. Magnitude and consequences of volatile release from the Siberian Traps. *Earth and Planetary Science Letters* 317, 363–373.

Braun, J., 2010. The many surface expressions of mantle dynamics. *Nature Geoscience* 3, 825–833.

Brookfield, M.E., Shellnutt, J.G., Qi, L., Hannigan, R., Bhat, G.M., Wignall, P.B., 2010. Platinum element group variations at the Permo-Triassic boundary in Kashmir and British Columbia and their significance. *Chemical Geology* 272, 12–19.

Bryan, S., Ernst, R., 2008. Revised definition of large igneous provinces (LIPs). *Earth-Science Reviews* 86, 175–202.

Campbell, I.H., 2005. Large igneous provinces and the mantle plume hypothesis. *Elements* 1, 265–269.

Campbell, I.H., Griffiths, R.W., 1990. Implications of mantle plume structure for the evolution of flood basalts. *Earth and Planetary Science Letters* 99, 79–93.

Chenet, A.-L., Fluteau, F., Courtillot, V., Gerard, M., Subbarao, K.V., 2008. Determination of rapid Deccan eruptions across the KTB using paleomagnetic secular variation: (1) results from 1200 m thick section in the Mahabaleshwar escarpment. *Journal of Geophysical Research* 113, B04101.

Coltice, N., Phillips, B.R., Bertrand, H., Ricard, Y., Rey, P., 2007. Global warming of the mantle at the origin of the flood basalts over supercontinents. *Geology* 35, 391–394.

Courtillot, V.E., Renne, P.R., 2003. On the age of flood basalt events. *Comptes Rendus Geoscience* 335, 113–140.

Courtillot, V., Gallet, Y., Rocchia, R., Féraud, G., Robin, E., Hofmann, C., Bhandari, N., Ghevariya, Z.G., 2000. Cosmic markers, $^{40}\text{Ar}/^{39}\text{Ar}$ dating and paleomagnetism of the KT sections in the Anjar Area of the Deccan large igneous province. *Earth and Planetary Science Letters* 182, 137–156.

Czamanske, G.K., Gurevich, A.B., Fedorenko, V., Simonov, O., 1998. Demise of the Siberian plume: paleogeographic and paleotectonic reconstruction from the prevolcanic and volcanic records, North-Central Siberia. *International Geology Review* 40, 95–115.

Dalrymple, G.B., Czamanske, G.K., Fedorenko, V.A., Simonov, O.N., Lanphere, M.A., Likhachev, A.P., 1995. A reconnaissance $^{40}\text{Ar}/^{39}\text{Ar}$ study of ore-bearing and related rocks, Siberian Russia. *Geochimica et Cosmochimica Acta* 59, 2071–2083.

Dobretsov, N.L., Vladimirov, A.G., Kruk, N.N., 2005. Permian–Triassic magmatism in the Altai-Sayan Fold System as a reflection of the Siberian superplume. *Doklady Earth Sciences* 400, 40–43.

Dobretsov, N.L., Kiriyashkin, A.A., Kiriyashkin, A.G., Vernikovskiy, V.A., Gladkov, I.N., 2008. Modeling of thermochemical plumes and implications for the origin of the Siberian Traps. *Lithos* 100, 66–92.

Elkins-Tanton, L.T., 2005. Continental magmatism caused by lithospheric delamination. In: Foulger, G.R., Natland, J.H., Presnall, D.C., Anderson, D.L. (Eds.), *Plates, Plumes, and Paradigms: Geological Society of America Special Paper*, 388, pp. 449–462.

Erwin, D.H., 1994. The Permo-Triassic extinction. *Nature* 367, 231–236.

Fedorenko, V.I., Lightfoot, P.C., Naldrett, A.J., Czamanske, G.K., Hawkesworth, C.J., Wooden, J.L., Ebel, D.S., 1996. Petrogenesis of the flood-basalt sequence at Noril'sk, North Central Siberia. *International Geology Review* 38, 99–135.

Fedoseev, G.S., Sotnikov, V.I., Rikhvanov, L.P., 2005. Geochemistry and geochronology of Permo-Triassic basites in the northwestern Altai-Sayan folded area. *Geologiya i Geofizika* 45, 289–302.

Feoktistov, G.D., 1978. *Petrology and Conditions for Formation of Trap Sills*. Nauka, Novosibirsk (168 pp. (in Russian)).

Foland, K.A., Xu, Y., 1990. Diffusion of ^{40}Ar and ^{39}Ar in irradiated orthoclase. *Geochimica et Cosmochimica Acta* 54, 3147–3158.

Glikson, A., 2004. Comment on "Bedout: a possible end-Permian impact crater offshore of Northwestern Australia". *Science* 306, 613.

Gradstein, F.M., Ogg, J.G., Schmitz, M., Ogg, G. (Eds.), 2012. *The Geologic Time Scale 2012*. 2-Volume Set, 1st edition. Elsevier.

Hallam, A., Wignall, P.B., 1997. *Mass Extinction and Their Aftermath*. Oxford University Press (328 pp.).

He, H.Y., Wang, X.L., Zhou, Z.H., Wang, F., Boven, A., Shi, G.H., Zhu, R.X., 2004. Timing of the Jiuftang Formation (Jehol Group) in Liaoning, northeastern China, and its implications. *Geophysical Research Letters* 31, L12605.

Heunemann, C., Krása, D., Soffel, H.C., Gurevitch, E., Bachtadse, V., 2004. Directions and intensities of the Earth's magnetic field during a reversal: results from the Permo-

- Triassic Siberian Trap basalts, Russia. *Earth and Planetary Science Letters* 218, 197–213.
- Hildebrand, R., Penfield, G.T., Kring, D.A., Pilkington, M., Camargo, A., Jacobsen, S.B., Boynton, W.V., 1991. Chicxulub crater: a possible Cretaceous/Tertiary boundary impact crater on the Yucatan Peninsula. *Geology* 19, 867–871.
- Ivanov, A.V., 2006. Systematic differences between U–Pb and $^{40}\text{Ar}/^{39}\text{Ar}$ dates: reasons and evaluation techniques. *Geochemistry International* 44, 1041–1047.
- Ivanov, A.V., 2007. Evaluation of different models for the origin of the Siberian Traps. In: Foulger, G.R., Jurdy, D.M. (Eds.), *Plates, Plumes and Planetary Processes: Geological Society of America Special Paper*, 430, pp. 669–691.
- Ivanov, A.V., Rasskazov, S.V., Feoktistov, G.D., He, H., Boven, A., 2005. $^{40}\text{Ar}/^{39}\text{Ar}$ dating of Usol'skii sill in the southeastern Siberian Traps large igneous province: evidence for long-lived magmatism. *Terra Nova* 17, 203–208.
- Ivanov, A.V., Demonerova, E.I., Rasskazov, S.V., Yasnygina, T.A., 2008. Low-Ti melts from the Southeastern Siberian Traps large igneous province: evidence for a water-rich mantle source? *Journal of Earth System Science* 117, 1–21.
- Ivanov, A.V., He, H., Yang, L., Nikolaeva, I.V., Paleskii, S.V., 2009. $^{40}\text{Ar}/^{39}\text{Ar}$ dating of intrusive magmatism in the Angara-Taseevskaya syncline and its implication for duration of magmatism of the Siberian Traps. *Journal of Asian Earth Sciences* 35, 1–12.
- Ivanov, A.V., Mazukabzov, A.M., Stanevich, A.M., Paleskii, S.V., Kozmenko, O.A., 2013. Testing the snowball Earth hypothesis for the Ediacaran. *Geology* (submitted for publication).
- Jourdan, F., Féraud, G., Bertrand, H., Watkeys, M.K., Renne, P.R., 2008. The $^{40}\text{Ar}/^{39}\text{Ar}$ ages of the sill complex of the Karoo large igneous province: implications for the Pliensbachian–Toarcian climate change. *Geochemistry, Geophysics, Geosystems* 9, Q06009.
- Kaiho, K., Kajiwar, Y., Nakano, T., Miura, Y., Kawahata, H., Tazaki, K., Ueshima, M., Chen, Z., Shi, G.R., 2001. End-Permian catastrophe by a bolide impact: evidence of a gigantic release of sulfur from the mantle. *Geology* 29, 815–818.
- Kamo, S.L., Czamanske, G.K., Krogh, T.E., 1996. A minimum U–Pb age for Siberian flood-basalt volcanism. *Geochimica et Cosmochimica Acta* 60, 3505–3511.
- Kamo, S.L., Czamanske, G.K., Amelin, Yu., Fedorenko, V.A., Davis, D.W., Trofimov, V.R., 2003. Rapid eruption of Siberian flood volcanic rocks and evidence for coincidence with the Permian–Triassic boundary and mass extinction at 251 Ma. *Earth and Planetary Science Letters* 214, 75–92.
- Kazanskii, A.Yu., Kazanskii, Yu.P., Saraev, S.V., Moskvina, V.I., 2000. The Permo-Triassic boundary in volcanosedimentary section of the West-Siberian Plate according to paleomagnetic data (from studies of the core from the Tyumenskaya superdeep borehole SD-6). *Geologiya i Geofizika* 41, 327–339 (in Russian).
- Keller, G., 2005. Impacts, volcanism and mass extinctions: random coincidence or cause and effect? *Australian Journal of Earth Sciences* 52, 725–757.
- Keller, G., Adatte, T., Pardo, A., Bajpai, S., Khosla, A., Samant, B., 2010. Cretaceous extinctions: evidence overlooked. *Science* 328, 974–975.
- King, S.D., Anderson, D.L., 1998. Edge-driven convection. *Earth and Planetary Science Letters* 160, 289–296.
- Koerber, C., Gilmour, L., Reimold, W.U., Claeys, P., Ivanov, B., 2002. End-Permian catastrophe by bolide impact: evidence of a gigantic release of sulfur from the mantle: comment. *Geology* 30, 855–856.
- Komarova, M.Z., 1968. On intrusion of granitoids in the Noril'sk region. *Geologiya i Geofizika* 5, 104–108 (in Russian).
- Koppers, A.A.P., 2002. ArArCALC–software for $^{40}\text{Ar}/^{39}\text{Ar}$ age calculations. *Computer and Geoscience* 28, 605–619.
- Kuzmichev, A.B., Pease, V.L., 2007. Siberian trap magmatism on the New Siberian Islands: constraints for Arctic Mesozoic plate tectonic reconstructions. *Journal of the Geological Society* 164, 959–968.
- Kyte, F.T., Smit, J., Wasson, J.T., 1985. Siderophile interelement variations in the Cretaceous–Tertiary boundary sediments from Caravaca, Spain. *Earth and Planetary Science Letters* 73, 183–195.
- Lee, C.-T.A., Wasserburg, G.J., Kyte, F.T., 2003. Platinum-group elements (PGE) and rhenium in marine sediments across the Cretaceous–Tertiary boundary: constraints on Re PGE transport in the marine environment. *Geochimica et Cosmochimica Acta* 67, 655–670.
- Leng, W., Zhong, S., 2010. Surface subsidence caused by mantle plumes and volcanic loading in large igneous provinces. *Earth and Planetary Science Letters* 291, 207–214.
- Lightfoot, P.C., Keays, R.R., 2005. Siderophile and chalcophile metal variations in flood basalts from Siberian Trap, Noril'sk region: implication for the origin of the Ni–Cu–PGE sulfide ores. *Economic Geology* 100, 439–462.
- Lin, S.C., van Keken, P.E., 2005. Multiple volcanic episodes of flood basalts caused by thermochemical mantle plumes. *Nature* 436, 250–252.
- Litasov, K., Ohtani, E., 2003. Stability of various hydrous phases in CMAS pyrolyte–H₂O system up to 25 GPa. *Physics and Chemistry of Minerals* 30, 147–156.
- Malitch, N.S., 1999. Editor-in-Chief. Geological map of Siberian platform and adjoining areas. Scale 1:1500000. VSEGEI, St-Petersburg.
- Masaitis, V.L., 1983. Permian and Triassic volcanism of Siberia. *Zapiski Vserossiiskogo Mineralogicheskogo Obshchestva* 4, 412–425 (in Russian).
- McDonough, W.F., Sun, S.-S., 1995. The composition of the Earth. *Chemical Geology* 120, 223–253.
- Min, K., Mundil, R., Renne, P.R., Ludwig, K.R., 2000. A test for systematic errors in $^{40}\text{Ar}/^{39}\text{Ar}$ geochronology through comparison with U/Pb analysis of a 1.1-Ga rhyolite. *Geochimica et Cosmochimica Acta* 64, 73–98.
- Mirnejad, H., Bell, K., 2006. Origin and source evolution of the Leucite Hills lamproites: evidence from Sr–Nd–Pb–O isotopic compositions. *Journal of Petrology* 47, 2463–2489.
- Mitchell, R.H., 1995. Melting experiments on a sanidine phlogopite lamproite at 4–7 GPa and their bearing on the source of lamproitic magmas. *Journal of Petrology* 36, 1455–1474.
- Müller, P.H., Neumann, P., Storm, R., 1979. *Tafeln der Mathematischen Statistik*. VEB Fachbuchverlag, Leipzig ((Russian edition), 278 pp.).
- Mundil, R., Brack, P., Meier, M., Rieber, H., Oberli, F., 1996. High resolution U–Pb dating of Middle Triassic volcanics: time-scale calibration and verification of tuning parameters for carbonate sedimentation. *Earth and Planetary Science Letters* 141, 137–151.
- Mundil, R., Ludwig, K.R., Metcalfe, L., Renne, P.R., 2004. Age and timing of the Permian mass extinctions: U/Pb dating of closed-system zircons. *Science* 305, 1760–1763.
- Nikolaeva, I.V., Paleskii, S.V., Koz'menko, O.A., Anoshin, G.N., 2008. Determination of rare earth and high field stress elements in standard geological samples by inductively coupled plasma mass-spectrometry (ICP-MS). *Geochemistry International* 46, 1085–1091.
- Paleskii, S.V., Nikolaeva, I.V., Koz'menko, O.A., Anoshin, G.N., 2009. Determination of platinum-group elements and rhenium in standard geological samples by isotope dilution with mass-spectrometric ending. *Journal of Analytical Chemistry* 64, 272–276.
- Pasyanos, M.E., 2010. Lithospheric thickness modeled from long-period surface wave dispersion. *Tectonophysics* 481, 38–50.
- Paton, M.T., Ivanov, A.V., Fiorentini, M.L., McNaughton, M.J., Mudrovskaya, I., Reznitskii, L.Z., Demonerova, E.I., 2010. Late Permian and Early Triassic magmatic pulses in the Angara-Taseeva syncline, Southern Siberian Traps and their possible influence on the environment. *Russian Geology and Geophysics* 51, 1012–1020.
- Pavlov, V.E., Fluteau, F., Veselovskiy, R.V., Fetisova, A.M., Latyshev, A.V., 2011. Secular geomagnetic variations and volcanic pulses in the Permian–Triassic traps of the Noril'sk and Maimecha-Kotui provinces. *Izvestiya-Physics of the Solid Earth* 47, 402–417.
- Pearson, D.G., Woodland, S.J., 2000. Carius tube digestion and solvent extraction/ion exchange separation for the analysis of PGEs (Os, Ir, Pt, Pd, Ru) and Re–Os isotopes in geological samples by isotope dilution ICP-mass spectrometry. *Chemical Geology* 165, 87–107.
- Peate, I.U., Bryan, S.E., 2008. Re-evaluating plume-induced uplift in the Emeishan large igneous province. *Nature Geoscience* 625–629.
- Peucker-Ehrenbrink, B., Jahn, B.-M., 2001. Rhenium–osmium isotope systematics and platinum group element concentrations: loess and the upper continental crust. *Geochemistry, Geophysics, Geosystems* 269. <http://dx.doi.org/10.1029/2001GC000172>.
- Priestley, K., McKenzie, D., 2006. The thermal structure of the lithosphere from shear wave velocities. *Earth and Planetary Science Letters* 244, 285–301.
- Racki, G., 2003. End-Permian mass-extinction: oceanographic consequences of double catastrophic volcanism. *Lethaia* 36, 171–173.
- Reichow, M.K., Saunders, A.D., White, R.V., Pringle, M.S., Al'mukhamedov, A.I., Medvedev, A.I., Kirda, N.P., 2002. $^{40}\text{Ar}/^{39}\text{Ar}$ dates from the West Siberian Basin: Siberian flood basalt province doubled. *Science* 296, 1846–1849.
- Reichow, M.K., Pringle, M.S., Al'mukhamedov, A.I., Allen, M.B., Andreichev, V.L., Buslov, M.M., Davies, C.E., Fedoseev, G.S., Fitton, J.G., Inger, S., Medvedev, A.Y., Mitchell, C., Puchkov, V.N., Safonova, I.Y., Scott, R.A., Saunders, A.D., 2009. The timing and extent of the eruption of the Siberian Traps large igneous province: implications for the end-Permian environmental crisis. *Earth and Planetary Science Letters* 277, 9–20.
- Renne, P.R., 1995. Excess ^{40}Ar in biotite and hornblende from the Noril'sk 1 intrusion, Siberia: implication for the age of Siberian Traps. *Earth and Planetary Science Letters* 131, 165–176.
- Renne, P.R., Basu, A.R., 1991. Rapid eruption of the Siberian Traps flood basalts at the Permo-Triassic boundary. *Science* 253, 176–179.
- Renne, P.R., Swisher, C.C., Deino, A.L., Karner, D.B., Owens, T.L., DePaolo, D.J., 1998. Intercalibration of standards, absolute ages and uncertainties in $^{40}\text{Ar}/^{39}\text{Ar}$ dating. *Chemical Geology* 145, 117–152.
- Ryabov, V.V., Shevko, A.Ya., Gora, M.P., 2001. Magmatic formations in Noril'sk region. *Trapp petrology*, vol. 1. Nonparel Publishers, Novosibirsk (408 pp. (in Russian)).
- Ryabov, V.V., Shevko, A.Ya., Gora, M.P., 2013. Trap magmatism and ore formation in Siberian Noril'sk region. *Trapp petrology*, vol. 1. Springer. <http://dx.doi.org/10.1130/G34345.1> (in press).
- Schulte, P., Alegret, L., Arenillas, I., Arz, J.A., Barton, P.J., Bown, P.R., Bralower, T.J., Christeson, G.L., Claeys, P., Cockell, C.S., Collins, G.S., Deutsch, A., Goldin, T.J., Goto, K., Grajales-Nishimura, J.M., Grieve, R.A.F., Gulick, S.P.S., Johnson, K.R., Kiessling, W., Koeberl, C., Kring, D.A., MacLeod, K.G., Matsui, T., Melosh, J., Montanari, A., Morgan, J.V., Neal, C.R., Nichols, D.J., Norris, R.D., Pierazzo, E., Ravizza, G., Rebolledo-Vieyra, M., Uwe Reimold, W., Robin, E., Salge, T., Speijer, R.P., Sweet, A.R., Urrutia-Fucugauchi, J., Vajda, V., Whalen, M.T., Willumsen, P.S., 2010. The Chicxulub asteroid impact and mass-extinction at the Cretaceous–Paleogene boundary. *Science* 327, 1214–1218.
- Self, S., Thordarson, T., Widdowson, M., 2005. Gas fluxes from flood basalt eruptions. *Elements* 1, 283–287.
- Shellnutt, J.G., Denyszyn, S.W., Mundil, R., 2012. Precise age determination of mafic and felsic intrusive rocks from the Permian Emeishan large igneous province (SW China). *Gondwana Research* 22, 118–126.
- Sheth, H.C., 2007. Large Igneous Provinces (LIPs): definitions, recommended terminology, and a hierarchical classification. *Earth-Science Reviews* 85, 117–124.
- Sheth, H.C., Pande, K., Bhutani, R., 2001. ^{40}Ar – ^{39}Ar ages of Bombay trachytes: evidence for a Palaeocene phase of Deccan volcanism. *Geophysical Research Letters* 28, 3513–3516.
- Sobolev, A.V., Hofmann, A.W., Kuzmin, D.V., Yaxley, G.M., Arndt, N.T., Chung, S.-L., Danyushevsky, L.V., Elliot, T., Frey, F.A., Garcia, M.O., Gurenko, A.A., Kamenetsky, V.G., Kerr, A.C., Krivolutskaya, N.A., Matvienkov, V.V., Nikogosian, I.K., Rocholl, A., Sigurdsson, I.A., Sushchevskaya, N.M., Teklay, M., 2007. The amount of recycled crust in sources of mantle-derived melts. *Science* 316, 412–417.
- Sobolev, A.V., Kuzmin, D.V., Krivolutskaya, N.A., 2009. Petrology of the parental melts and mantle sources of Siberian Trap magmatism. *Petrology* 17, 253–286.

- Sobolev, S.V., Sobolev, A.V., Kuzmin, D.V., Krivolutskaya, N.A., Petrunin, A.G., Arndt, N.T., Radko, V.A., Vasiliev, Y.R., 2011. Linking mantle plumes, large igneous provinces and environmental catastrophes. *Nature* 477, 312–316.
- Spell, T.L., McDougall, I., 2003. Characterization and calibration of $^{40}\text{Ar}/^{39}\text{Ar}$ dating standards. *Chemical Geology* 198, 189–211.
- Steiger, R.H., Jäger, E., 1977. Subcommittee on geochronology: convention on the use of decay constants in geo- and cosmochronology. *Earth and Planetary Science Letters* 36, 359–362.
- Steiner, M.B., 2006. The magnetic polarity time scale across the Permian–Triassic boundary. In: Lucas, S.G., Cassinis, G., Schneider, J.W. (Eds.), *Non-marine Permian Biostratigraphy and Biochronology: Geological Society (London) Special Publication*, 265, pp. 15–38.
- Sun, Y.D., Lai, X.L., Wignall, P.B., Widdowson, M., Ali, J.R., Jiang, H.S., Wang, W., Yan, C.B., Bond, D.P.G., Veldrine, S., 2010. Dating the onset and nature of the Middle Permian Emeishan large igneous province eruptions in SW China using conodont biostratigraphy and its bearing on mantle plume uplift models. *Lithos* 119, 20–33.
- Svensen, H., Planke, S., Malthe-Sorensen, A., Jamtveit, B., Myklebust, R., Eidem, T., Rey, S.S., 2004. Release of methane from a volcanic basin as a mechanism for initial Eocene global warming. *Nature* 429, 542–545.
- Svensen, H., Planke, S., Polozov, A.G., Schmidbauer, N., Corfu, F., Podladchikov, Y.Y., Jamtveit, B., 2009. Siberian gas venting and the end-Permian environmental crisis. *Earth and Planetary Science Letters* 277, 490–500.
- Svensen, H., Corfu, F., Polteau, S., Hammer, Ø., Planke, S., 2012. Rapid magma emplacement in the Karoo large igneous province. *Earth and Planetary Science Letters* 325, 1–9.
- Tohver, E., Lana, C., Cawood, P.A., Fletcher, I.R., Jourdan, F., Sherlock, S., Rasmussen, B., Trindade, R.I.F., Yokoyama, E., Souza Filho, C.R., Marangoni, Y., 2012. Geochronological constraints on the age of a Permo-Triassic impact event: U–Pb and $^{40}\text{Ar}/^{39}\text{Ar}$ results for the 40 km Araguainha structure of central Brazil. *Geochimica et Cosmochimica Acta* 86, 214–227.
- Travin, A.V., Yudin, D.S., Vladimirov, A.G., Khromykh, S.V., Volkova, N.I., Mekhonoshin, A.S., Kolotilina, T.B., 2009. Thermochronology of the Chernorud granulite zone, Ol'khon Region, Western Baikal area. *Geochemistry International* 47, 1107–1124.
- Vasil'ev, Yu.R., Zolotukhin, V.V., Feoktistov, G.D., Prusskaya, S.N., 2000. Evaluation of the volumes and genesis of Permo-Triassic trap magmatism of the Siberian platform. *Geologiya i Geofizika* 41, 1696–1705 (in Russian).
- Venkatesan, T.R., Kumar, A., Gopalan, K., Al'mukhamedov, A.I., 1997. ^{40}Ar – ^{39}Ar age of Siberian basaltic volcanism. *Chemical Geology* 138, 303–310.
- Vernikovskaya, A.E., Vernikovskiy, V.A., Matushkin, N.Yu., Romanova, V.I., Berejnaya, N.G., Larionov, A.N., Travin, A.V., 2010. Middle Paleozoic and Early Mesozoic anorogenic magmatism of the South Yenisei Ridge: first geochemical and geochronological data. *Russian Geology and Geophysics* 51, 548–562.
- Vernikovskiy, V.A., Pease, V.L., Vernikovskaya, A.E., Romanov, A.P., Gee, D.G., Travin, A.V., 2003. First report of early Triassic A-type granite and syenite intrusions from Taimyr: product of the northern Eurasian superplume? *Lithos* 66, 23–36.
- Vladimirov, A.G., Kozlov, M.S., Shokal'skii, S.P., Khalilov, V.A., Rudnev, S.N., Kruk, N.N., Vystavnoi, S.A., Borisov, S.M., Berezhevnikov, Y.K., Metsner, A.N., Babin, G.A., Mamlin, A.N., Murzin, O.M., Nazarov, G.V., Makarov, V.A., 2001. Major epochs of the intrusive magmatism of Kuznetsk Alatau, Altai, and Kalba (from U–Pb isotope dates). *Geologiya i Geofizika* 42, 1157–1178.
- Vrublevskii, V.V., Gertner, I.F., Polyakov, G.V., Izokh, A.E., Krupchatnikov, V.I., Travin, A.V., Voitenko, N.N., 2004. Ar–Ar isotopic age of lamproite dikes of the Chua complex, Gornyi Altai. *Doklady Earth Sciences* 399A, 1252–1255.
- Walderhaug, H.J., Eide, E.A., Scott, R.A., Inger, S., Golionko, E.G., 2005. Paleomagnetism and $^{40}\text{Ar}/^{39}\text{Ar}$ geochronology from the South Taimyr igneous complex, Arctiv Russia: a Middle-Late Triassic magmatic pulse after Siberian flood-basalt volcanism. *Geophysical Journal International* 163, 501–517.
- Wooden, J.L., Czamanske, G.K., Fedorenko, V.A., Arndt, N.T., Chauvel, C., Bouse, R.M., King, B.-S.W., Knight, R.J., Siems, D.F., 1993. Isotopic and trace-element constraints on mantle and crustal contributions to characterization of Siberian continental flood basalts, Noril'sk area, Siberia. *Geochimica et Cosmochimica Acta* 57, 3677–3704.
- Wooley, A.R., Bergman, S.C., Edgar, A.D., Le Bas, M.J., Mitchell, R.H., Rock, N.M.S., Smith, B.H.S., 1996. Classification of lamprophyres, lamproites, kimberlites, and the calcilic, melilitic, and leucitic rocks. *The Canadian Mineralogist* 34, 175–186.
- Zolotuhin, V.V., Vilenskii, A.M., Dyuzhikov, O.A., 1986. Basalts of the Siberian Platform: Peculiarities of Geology, Composition and Genesis of the Permo-Triassic Effusives. Nauka, Novosibirsk (245 pp. (in Russian)).